STRUCTURE AND ADSORPTION AT THE WATER / CARBON TETRACHLORIDE INTERFACE

by

Tammy Baisley

B.Sc., Mount Allison University, Sackville, New Brunswick, 1995

THESIS SUBMITTED IN PARTIAL FULFILLMENT OF

THE REQUIREMENT FOR THE DEGREE OF

MASTER OF SCIENCE

in the Department

of

Chemistry

SIMON FRASER UNIVERSITY

August 1997

APPROVAL

Name: Tammy Baisley

Degree: Master of Science

Title of thesis: Structure and Adsorption at the Water / Carbon Tetrachloride Interface

Examining Committee:

Chairperson: Dr. Ian Gay, Professor

Dr. Gary Leach, Assistant Professor
Senior Supervisor

Dr. George Agnes, Assistant Professor

Dr. Paul Percival, Professor

Dr. Ross Hill, Associate Professor
Internal Examiner

Date Approved: August 14, 1997.

ABSTRACT

The interface specific nonlinear optical technique of second harmonic generation has been used to examine the structure of and adsorption at the neat water / carbon tetrachloride liquid-liquid interface. These studies yield information about the energetics of interfacial species, and provide a description of this complex interface on the molecular scale.

Polarization dependent studies were executed on the neat water / carbon tetrachloride interface using second harmonic generation. From these studies the water / carbon tetrachloride interface susceptibilities were extracted. These experimentally determined values indicate that the averaged orientation of the interfacial water molecules is one in which the dipole of the molecules lies parallel to the interface.

Second harmonic generation was also employed in the detection of monolayer coverages of p-nitroaniline molecules at the water / carbon tetrachloride interface. These studies provide a measure of the adsorption energetics and averaged molecular orientation of this organic probe molecule at the interface. P-nitroaniline was found to have a Gibbs free energy of adsorption of -9.48 kcal/mol (-41.2 kJ/mol), indicating a relatively strong preference for residing at the interface over the bulk solution. It was also found that the interfacial p-nitroaniline molecules possessed a strong orientational anisotropy indicating a preferred orientation at the interface. This orientation corresponds to the symmetry axis of p-nitroaniline having an averaged orientation angle of 48° ± 2°, with respect to the interface normal. The pH dependence of p-nitroaniline was also investigated in order to examine the adsorption energetics of the p-nitroanilinium ion. It was found that the averaged orientation angle did not

change upon protonation but the Gibbs free energy of adsorption increased to -7.75 kcal/mol (-32.4 kJ/mol).

As well a characterization of the water / carbon tetrachloride interface upon adsorption of a series of small ions was undertaken. The Gibbs free energy of adsorption of the ions was determined to depend on the size of the ion and scale with their size. The ions that were investigated were hydrogen, lithium, and sodium. The Gibbs free energies of adsorption for these ions were all small positive numbers, indicating a preference for being in solution. The second harmonic response in the case of small ion adsorption is the result of an electric field induced second harmonic process and was also effected by the reorientation of water molecules to solvate these ions.

To my parents, Fred and Yvette Baisley

ACKNOWLEDGMENTS

I wish to thank my senior supervisor, Dr. Gary Leach, for his ongoing guidance, attention and patience throughout my studies.

I would like to thank the members of my group, Zhihong Zhao, Tatyana Kiktyeva and Dimitry Star, for their help and friendship.

I wish to express my gratitude to the members of my supervisory committee, Drs. George Agnes and Paul Percival, for their time and attention.

I would also like to thank Dr. Ross Hill and his group for their input and helpful discussions during group meetings.

I would also like to express my gratitude to Dr. Paul Beattie for his informative discussions.

Special thanks goes to Michael Belyea for his patience, support and encouragement throughout my studies.

The generous financial support from the Department of Chemistry at Simon Fraser University and Dr. Gary Leach's research funds is gratefully acknowledged.

TABLE OF CONTENTS

LIST OF FIGURES

Chapter 1: Introduction

1.1) Liquid - Liquid Interfaces

Interfaces are boundaries that separate two bulk media. When two chemically different immiscible liquids are combined, a liquid-liquid interface is formed. The interface has unique chemical and physical properties that are different then the bulk media. These differences are caused by the asymmetry in forces that molecules encounter there. This asymmetry leads to a different arrangement of molecules at the interface than would be found in the bulk and can produce a net orientation of molecules and influence chemical reactions that occur there. As a result of these unique solvation and orientation properties, reactions at interfaces can occur with different rates and to differing extents than they would in the bulk phases. [1]

The transport of chemical species across interfaces is important not only from the fundamental point of view of understanding chemical reactions that occur there but are also of interest due to their importance in biological systems and environmental issues. For example, liquid - liquid interfaces provide biologists and biochemists with a laboratory model of biomembranes, [2] and air / water as well as aqueous / solid interfaces can be used to help us understand the effects of pollutants on rivers, lakes and in soils. [1] The first step

to understanding the kinetics and dynamics of reactions at interfaces is to obtain a complete understanding of the orientation and organization of solute and solvent molecules which reside there.

Despite the desire to understand interfacial processes on the molecular scale attempts to observe these processes directly through spectroscopic means have been greatly impeded by the difficulty in separating the optical response of the solute molecules at the interface from the overwhelmingly large number of solute molecules in the adjacent bulk media. [1] A typical concentration of molecules forming a closed packed monolayer would be on the order of 10^{14} molecules/cm^2. Whereas a 1 mM solution would have on the order of 10^{19} molecules/cm^3. A nonlinear optical technique called surface second harmonic generation (SHG), the primary tool used in the work described here, can overcome this problem. A brief description of this nonlinear optical technique follows.

1.2) Optical Second Harmonic Generation

In an atomic or molecular system, the distance between the charges changes when an electric field is applied. In other words a polarization has occurred. [3] If the polarization is completely linear, for example, if the field strength increases by a factor of five then the polarization increases by the same factor, the polarization is described by linear response theory:

$$P = \chi^{(1)} E \quad (1)$$

where E is the intensity of the electric field and $\chi^{(1)}$ is the linear or first order susceptibility. [4] This linear response of the medium to applied electric fields is observed over a broad range of electric field strengths. However, in the case of large electric fields (comparable to the field binding electrons to the nucleus) such as those applied with an intense laser beam, the response can be nonlinear and additional parameters must be introduced to describe the polarization accurately:

$$P = \chi^{(1)}E + \chi^{(2)}EE + \chi^{(3)}EEE + \ldots \quad (2)$$

The $\chi^{(2)}$ term is the second order nonlinear susceptibility term, typically a factor of 10^6 smaller then $\chi^{(1)}$. This term can only occur in the absence of inversion symmetry. [3] By symmetry, if a medium is isotropic then $\chi^{(2)} = 0$. When an interface is formed between two bulk phases of matter each with $\chi^{(2)} = 0$, the interface possesses a $\chi^{(2)}$ because of its inherent lack of symmetry.

The nonlinear optical technique employed for our studies is second harmonic generation. Second Harmonic Generation (SHG) is the nonlinear optical process that converts an input of two photons of frequency ω to an output of one photon of frequency 2ω and requires a medium in which $\chi^{(2)} \neq 0$ to do so. Since the interface between centrosymmetric bulk media possesses a nonzero $\chi^{(2)}$, only the molecules participating in the asymmetry of the interface will give rise to a second harmonic nonlinear optical response. A scheme of this process can be seen in figure 1.1. Figure 1.1a) represents an input of two photons of

frequency ω and an output of one photon of frequency 2ω. This process is not to be confused with absorption followed by emission, SHG is a coherent light scattering process. Figure 1.1b) is a representation of how the experiment is carried out. An input beam of light with frequency ω strikes the interface generating an output with frequency 2ω.

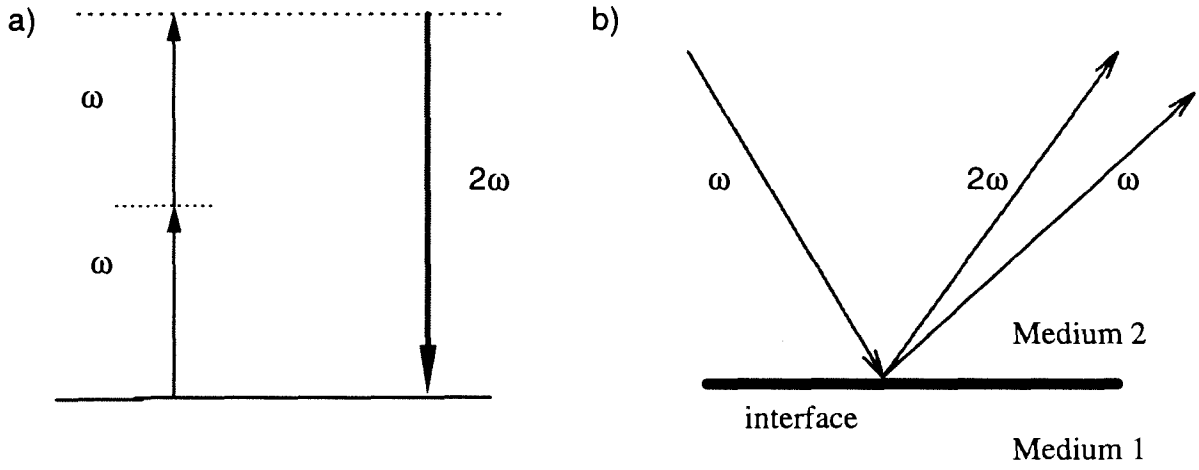

Figure 1.1: a) and b) Schematic representations of SHG

With its submonolayer sensitivity, almost immediate response time, and its surface specificity, SHG has begun to be recognized as a valuable tool to study a variety of surfaces and interfaces. This technique has been used as a surface analytical probe to detect submonolayer coverages [5], to determine the molecular orientation at a variety of interfaces [6], and to study dynamic processes at interfaces [7].

Second harmonic generation can be categorized in terms of the nature of the interface susceptibility giving rise to the nonlinear response. In addition to a second harmonic (SH) signal being generated by the breaking of symmetry which defines the interface, by the nonlinear polarizability of molecules from either or both of the bulk phases which reside at the interface, it can also be generated in other ways. It could be generated by an electric field during adsorption of charged species at the interface or by external means, or by the presence of species with nonlinear polarizabilities specifically adsorbed at the interface. In the absence of significant nonlinear polarizability, SHG resulting from interfacial discontinuities alone is extremely weak. The signal will increase when charged species are placed in the system. This case is complicated by the fact that the signal has two components, the molecular component arising from the molecule that carries the charge and the charge component arising from the formation of dipoles. [8] These sorts of studies are usually done on charged molecules with SHG and electrochemical techniques. In the case of an organic molecule at the interface, the size of the signal is usually determined by the molecular hyperpolarizability, β, of that molecule and can easily dominate any contributions from the neat interface. [9] The β is proportional to

$$\beta \propto \left(\mu_{ee} - \mu_{gg}\right)\frac{\mu_{ge}^{2}}{E_{ge}^{2}} \qquad (3)$$

where g is the ground state, e is the excited state, μ_{ge} is the transition dipole between the ground state and the excited state, μ_{ee} is the permanent dipole of

the excited state, μ_{gg} is the permanent of the ground state and E_{ge} is the transition energy between the ground state and the excited state. The terms of this equation are a function of the molecular structure and have their own characteristic maxima. To obtain a large signal, a balance of a large difference in the dipoles between the ground state and the excited state, a large oscillator strength (μ^2_{ge}) and a small transition energy must be obtained. A molecule will have a large β if it has a donor group on one end of the molecule, an acceptor group on the other and a bridging group attaching them. In general, β increases with increasing donor and acceptor strength. [9]

The next few paragraphs are dedicated to providing an overview of the work that has been done at a variety of liquid interfaces. This discussion will be divided into a description of the adsorption and orientation of small organic molecules and surfactants, chemical equilibrium studies and chemical reactions at interfaces.

1.3) Previous Studies

The adsorption of small organic molecules at a variety of interfaces have been studied using SHG to determine the adsorption strength and the surface

coverage. The orientation of these molecules has also been investigated. These experiments have determined that for the adsorption of small organic molecules the Gibbs free energies of adsorption ranges from -2 to -10 kcal/mol. For example, Heinz *et. al.* [10] studied p-nitrobenzoic acid at the ethanol-silica interface. They point out the saturation behavior in surface coverage after a monolayer has been formed and find the Gibbs free energy of adsorption ($\Delta G°_{ads}$) from the isotherm to be -8.0 kcal/mole. Corn *et al* [11-13] have done similar work with p-nitrophenol at the silica-chloroform interface and obtained a ($\Delta G°_{ads}$) of approximately -3.5 kcal/mole. Bhattacharya *et. al.* [14,15] have used SHG to study the adsorption of alkylanilines and alkylphenols and their ions at the air/water interface. The free energies of adsorption were determined. They concluded that the driving force for interfacial adsorption of these molecules increased with carbon chain length. To be consistent with the literature all results will be given in kcal/mol where 1 cal = 4.184 joules.

SHG polarization studies have been performed at various liquid interfaces. For example, Conboy *et. al.* [16] used second harmonic generation in a total internal reflection geometry to study a series of neat water / *n*-alkane interfaces. The examination of the interface susceptibilities there yielded the interesting result that water / alkane interfaces are less ordered when the carbon chain has an odd number of carbons than when the carbon chain has an even number of carbons.

Some larger organic molecules, namely surfactants have also been widely investigated at a variety of interfaces. These studies have provided invaluable

information about surfactant behavior at interfaces. One study was performed by Corn *et. al.* [11-13] who investigated the adsorption of neutral and cationic surfactants at the water/1,2-dichloroethane interfaces. Rasing *et. al.* [17] reported some interesting experiments in which they examined the averaged molecular orientation of sodim-dodecylnapthalene-sulfonate (SDNS) at the water-air interface. They found that the orientation of SDNS varied smoothly and tilted more toward the surface normal with increasing surface pressure, approaching a limiting angle of 30° with respect to the surface normal.

Investigations of chemical equilibria at liquid-liquid interfaces using second harmonic generation have also been performed. In one such study, Eisenthal *et. al.* [1, 18] investigated the acid-base equilibrium between p-nitrophenol and its anion at the air/water interface. These studies concluded that the anion does not reside at the surface but prefers the bulk water. Further, in a study of the pH dependence of hexadecylanilinium ($CH_3(CH_2)_{15}C_6H_4NH_3^+$), the interfacial pK_a was found to be 3.6, a factor of 50 more acidic than the bulk equilbria.

SHG studies of interfacial chemical reactions have been limited to relatively simple chemical processes. Goh *et. al.* [19] performed the first photo-isomerization at a liquid interface. They studied 3,3 diethyloxadi-carbocyanide iodide (DODCI) at the air/water interface. They concluded that the lifetime of the cis isomer is 220 ps at the interface compared to 520 ps in the bulk. This is an example of a reaction which has a different rate at the interface than it does in the bulk. This result indicates that the barrier to isomerization in the bulk is less than at the interface. Meech and Yoshihara [20, 21] studied photo-isomerization of

malachite green at a diethyl ether/quartz interface and at the air/quartz interface. In this case they found that the time scale for photoisomerizations were approximately the same and on the order of 40ps.

1.4) Focus of the Study

Few studies have been performed at liquid-liquid interfaces despite its importance and widespread interest in a variety of fields. This investigation uses SHG as a spectroscopic tool in the characterization of the neat water / carbon tetra chloride interface, in the detection of monolayer coverages of small organic molecules at interface, in the determination of their averaged molecular orientation, and in an investigation of adsorption processes that occur at the interface.

We have investigated the neat water / carbon tetrachloride interface with second harmonic generation, using polarization techniques to extract the interface susceptibilities. As well, at this interface, p-nitroaniline (pNA) and its cation were probed in terms of the averaged orientation of each, the adsorption strength and the surface coverage. Also, a characterization of the water / carbon tetrachloride interface upon addition of small ions was undertaken. The ions that were investigated were hydrogen, lithium, and sodium.

These experiments and their results will be discussed in detail in the next few chapters. Chapter two will describe the experimental setup and the

preparation of the interfaces. Chapter three focuses on the characterization of the neat water / carbon tetrachloride (CCl_4) interface. Then chapter four discusses the adsorption and energetics of the interfacial pNA molecules. Chapter five provides details on the adsorption process of hydrogen, lithium and sodium ions. Finally a brief conclusion is provided in chapter six.

Chapter 2: Experimental

This chapter provides a detailed description of the experimental apparatus and sample preparation procedures used in carrying out the experiments discussed in this thesis. Section 2.1 describes in detail the optical setup used for the optical second harmonic generation studies. Section 2.2 outlines another technique used in the characterization of the interface, ultraviolet adsorption spectroscopy. Finally, section 2.3 gives a discussion about the sample preparation and chemicals used.

2.1) Optical Setup

The adsorption process, the averaged orientation of adsorbed species and the pH dependence of molecules at the water - CCl_4 interface have been studied using SHG. The laser system used for these studies consists of four parts, as represented schematically in figure 2.1. A mode-locked Ti:sapphire laser is pumped by using 7 Watts of a 10 Watt argon ion laser (Spectra Physics, Beamlock 2060-10SA),. The Ti:sapphire laser (Spectra Physics, Tsunami 3960) produces an 82 MHz pulse train, tunable from approximately 750 - 850 nm with an 80 fs pulse duration. Part of this pulse train is then amplified in a chirped pulse regenerative amplifier (Positive Light, Spitfire) which is pumped by a Q-switched Nd:YLF laser (Positive Light, Merlin) which operates at a 1 kHz

repetition rate. The average power of the laser system is 1 W. This system can produce 100 fs pulses each with 1 mJ of energy, thus having a peak power of 10 GW and is tunable over a range of 750 - 850 nm. Pulses with such high peak intensities can damage the interfaces that are being investigated, therefore less than 150 mW of the available laser power was used.

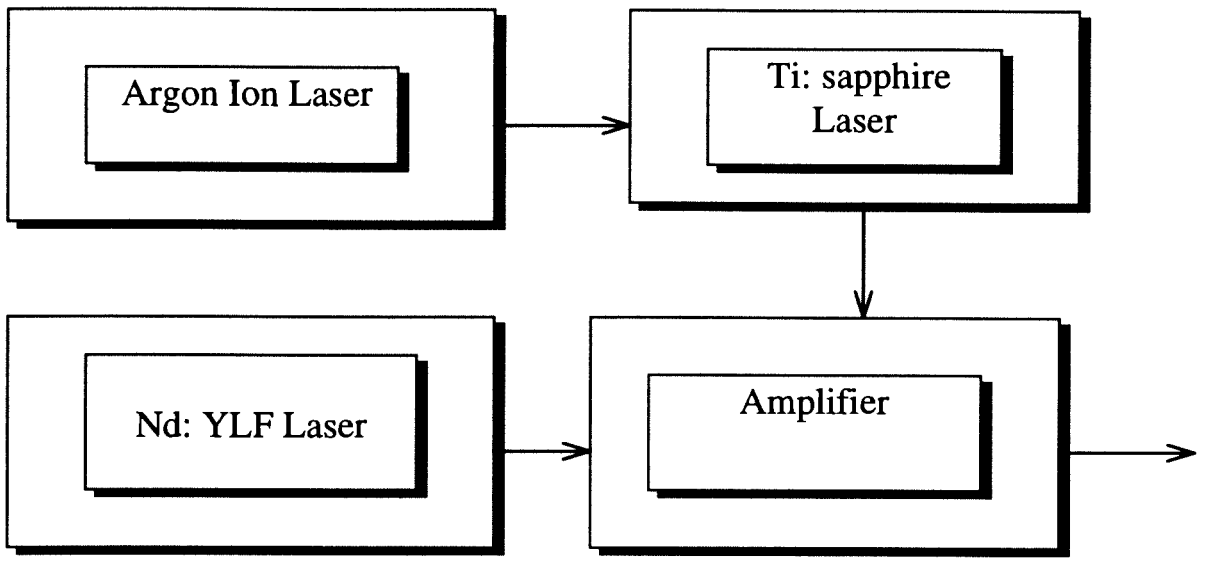

Figure 2.1: Schematic representation of the laser system.

The polarization of this laser beam was controlled by a quartz zero-order half wave plate (CVI Laser). The beam then passes through a filter (CVI Laser) to cut off any SH light that was generated from the optics before the sample. The laser light is then sent to the sample cell where it enters the CCl_4 side of the cell (see figure 2.2). The sample cell (see figure 2.2) was designed so that the laser light would undergo total internal reflection (TIR). The SH light generated

liquid - liquid interface then propagates along the interface due to the total internal reflection geometry.

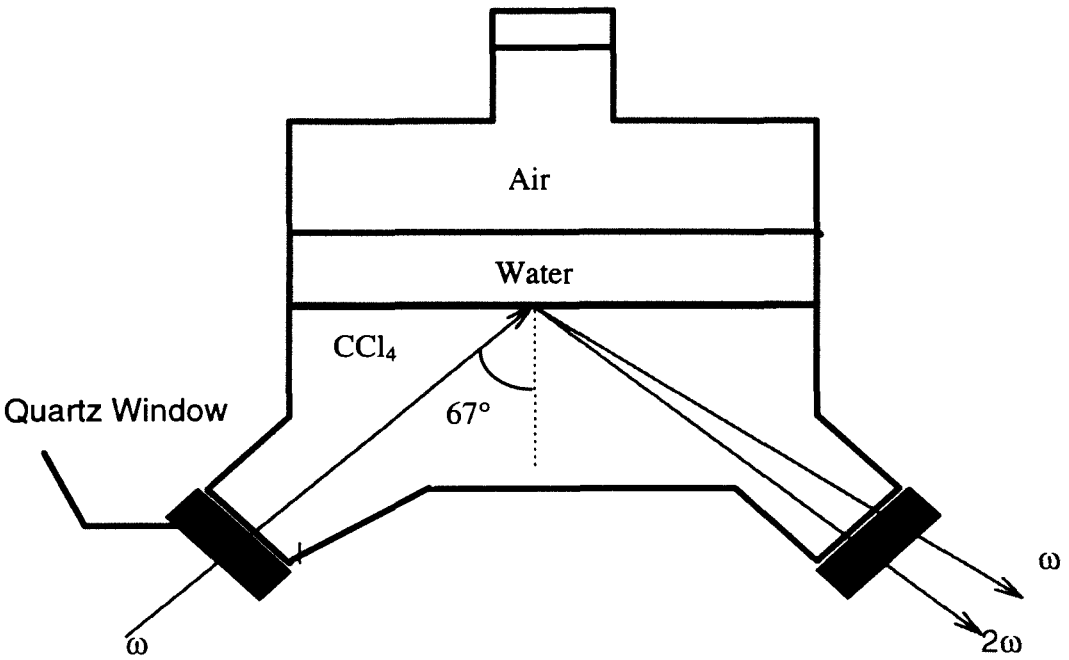

Figure 2.2: Schematic representation of the sample cell

The TIR optical geometry is used to enhance the SH signal. As the light approaches total internal reflection geometry the reflected beam grows stronger while the transmitted beam grows weaker until the transmitted beam finally vanishes and all the light is reflected. The total internal reflection geometry is employed because it has been shown to lead to enhancement in signal levels of

up to two orders of magnitude. TIR produces an evanescent wave which propagates along the interface for distances on the order of the optical wavelength.[22] This increases the length of interaction between the incident light and interfacial molecules responsible for SHG. The result is signals much larger than those obtained in a more conventional external reflection geometry. The index of refraction of CCl_4 is 1.460 and water is 1.332. These refracted indices lead to a total internal reflection angle of 67° with respect to the interface normal, as indicated in figure 2.2.

After passing through the sample cell, the fundamental and the second harmonic light are spatially separated. Due to the wavelength difference they propagate at slightly different angles. The second harmonic light then passes through a Glan-Taylor polarization analyzer (CVI Laser) allowing selective polarization. The SH signal is then focused into the entrance of a 0.25 meter monochrometer (CVI Laser, Digikrom 240). The light is then collected with a photomultiplier tube (Hammamatsu Systems, SR 240). The photomultiplier tube (PMT) signal is then sent to the gated electronics (SRS) where it is averaged and directed to a microcomputer for storage and analysis. See figure 2.3 for a schematic representation of the experimental setup.

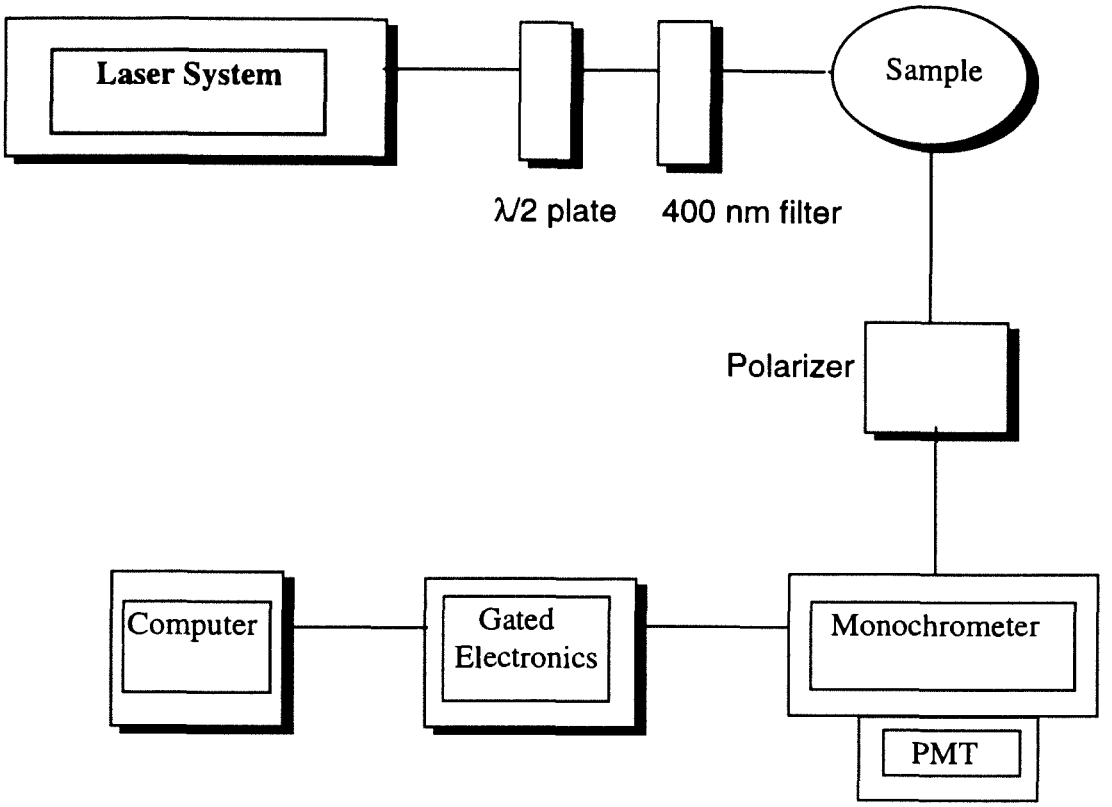

Figure 2.3: Experimental setup for optical studies

2.2) Ultraviolet Adsorption Spectroscopy

Ultraviolet absorption spectroscopy was used to determine what wavelengths should be chosen for the optical experiments. A Hewlett Packard HP8452 Diode Array Spectrophotometer, was used to determine the wavelengths that the molecules absorbed in CCl_4. A knowledge of this is necessary to determine what wavelengths will be used for the nonlinear optical experiments, due to the low signal levels inherent with this type of experiment.

SHG studies involving organic adsorbates are usually conducted under circumstances of resonance enhancement. The largest signals would come from using wavelengths of fundamental or second harmonic light that are resonant with an energy level of the molecule. Figure 2.4 represents such a scenario. Case a) illustrates molecular resonance enhancement occurring at the fundamental wavelength, ω, where g is the ground state and n is a single excited state. Case b) represents molecular resonance enhancement occurring at the second harmonic wavelength.

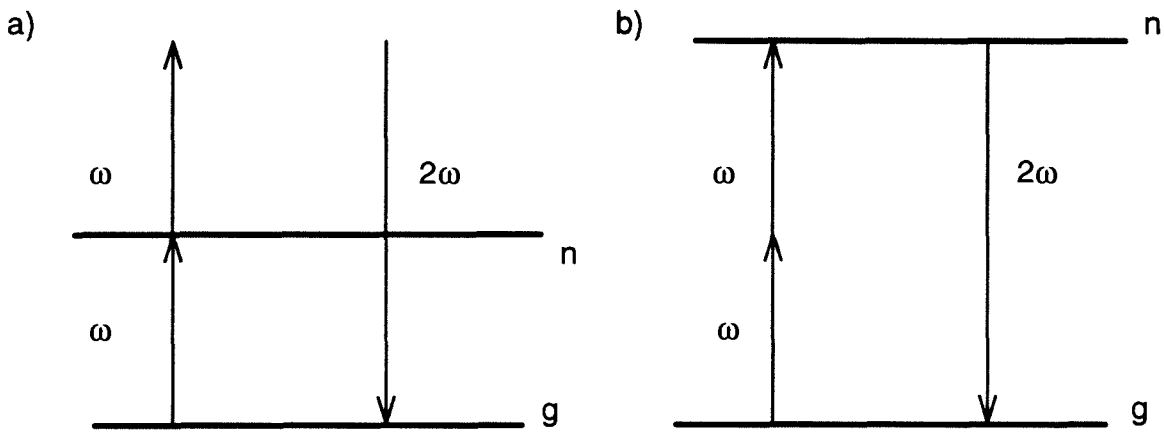

Figure 2.4 : Schematic representation of a two state model for resonant molecular SHG

Due to the geometry of the sample cell (see figure 2.3), a wavelength outside the absorbance of those molecules must be chosen or the SH signal produced at the interface would be entirely absorbed by the solution before it could reach the

detector. Figure 2.5 shows the absorption spectrum of pNA in CCl_4. The maximum absorbance occurs at 330 nm. Our experiments were carried out using a fundamental wavelength of 814 nm so that the SH signal appearing at 407 nm would not be adsorbed.

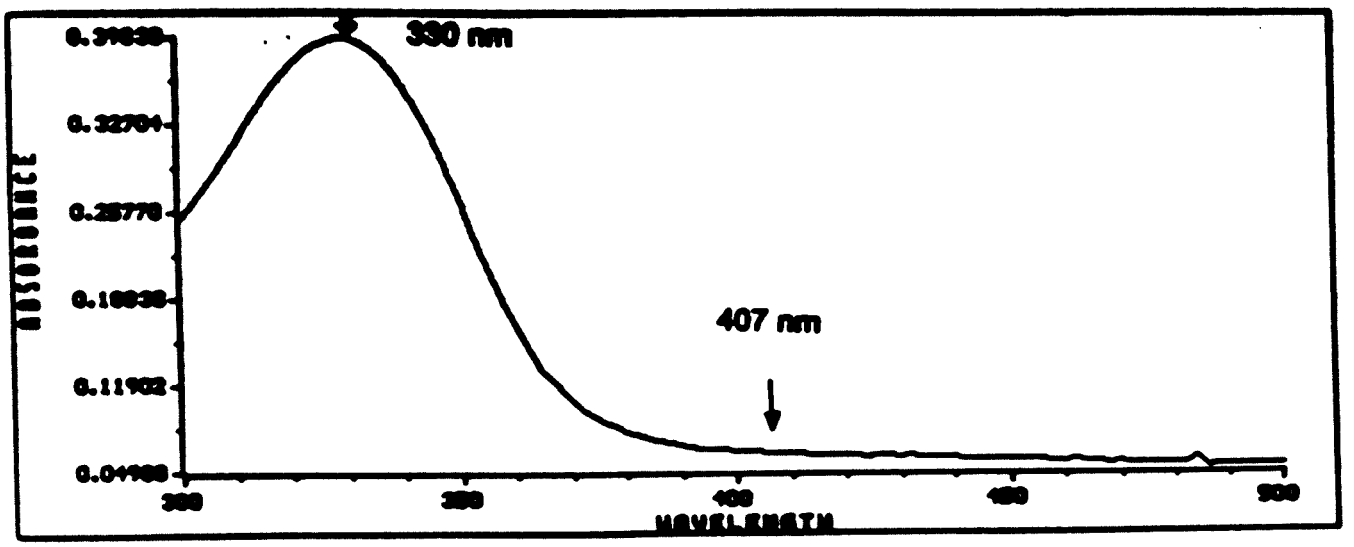

Figure 2.5 : Absorption spectrum of pNA in CCl_4. Maximum absorbance is at 330 nm, as labeled. The nonlinear optics experiments were carried out with second harmonic signal appearing at 407nm.

2.3) Sample Preparation

Ultra pure (Millipore) water, with a resistivity of 18.2 MΩ/cm, and carbon tetrachloride (CCl_4), manufactured by Mallinckrodt with a purity of 99.8% (used as received), were used to make the liquid-liquid interface. The densities of CCl_4 and water are 1.59 g/ml and 0.998 g/ml respectively. The sample cell was cleaned by allowing it to soak overnight in concentrated sulfuric acid (Anachemia, 98%) then rinsed thoroughly in ultrapure water and dried. Finally, it was rinsed several times with carbon tetrachloride before the CCl_4 for the interface was deposited in the cell. The molecules of interest were dissolved in the ultrapure water and then gently poured onto the CCl_4. The molecules of interest were p-nitroaniline (MCB reagents, 99%), hydrochloric acid (Anachemia, 98.9%), sodium hydroxide (Fisher 99%), sodium chloride (Anachemia, 99%) and lithium chloride (J. T. Chemical Co., 98.6%). All molecules were used as received.

Chapter 3: Investigation of the Neat Water / Carbon Tetrachloride Interface

3.1) Introduction

We begin our study of the water / CCl_4 interface by investigating the structure of the neat interface. Using the surface specific nonlinear optical technique of SHG, we have studied the orientation of the water molecules at the water / CCl_4 interface.

Water is known to form hydrogen bonds with surrounding water molecules. The hydrogen bond is an electrostatic interaction between hydrogen and electronegative elements, in this case oxygen. The strength of a hydrogen bond is between 10 and 40 kJ/mol. [23] In ice, each water molecule can participate in four hydrogen bonds, two involving its own hydrogen atoms and two involving the oxygens lone pair electrons, in a tetrahedral shape. [23] For liquid water, the molecules participate in 3 - 3.5 hydrogen bonds. This decrease is due to the fact that the structure is more labile and disordered. [23] When water molecules come into contact with non-polar molecules, any way they orient themselves, some of their hydrogen bonds must break. When a molecule is not very soluble in water, like a hydrocarbon, it is characterized by an unfavorable free energy of solubilization which is mainly entropic. To dissolve a molecule in water causes

the breaking of hydrogen bonds, resulting in an increase in entropy. The immiscibility of molecules with water and the entropic nature of this immiscibility is called the hydrophobic effect. [23]

The case of water forming an interface with a nonpolar liquid, like CCl_4, is an extreme example of this. On the CCl_4 side of the interface, no neighboring molecules can be hydrogen bonded. For the water molecules one may expect that the most energetically favorable situation would be one in which the orientation of the interfacial water molecules involved the breaking of as few hydrogen bonds as possible.

With this in mind, the results of the orientation studies of the water molecules at the water / CCl_4 interface will be presented and discussed in this chapter.

3.2) Experimental Procedure

The experimental setup is as per section 2.2.2). The orientation is determined by monitoring the SH signal while varying the polarization of the electric field of the input laser with the half wave plate. The reflected SH light then passes through a polarizer set to pass either s-polarized (0° with respect to the plane of incidence) or p-polarized light (90° with respect to the plane of incidence) before being spectrally dispersed and sent to a detector. For each

sample, data was recorded for each of the s- and p- polarized SH response. These curves were fitted with theoretical fits and the interface susceptibilities were determined as outlined below. The next section will provide a brief description of the fitting procedure. This will be discussed in more detail in chapter 4.

3.3) Orientation Theory and Fitting Procedure

The intensity of the second harmonic signal is proportional to the squares of the second order nonlinear susceptibility of the molecules, $\chi^{(2)}$, and the intensity of the incident laser light, $I(\omega)$, as indicated in equation 4.

$$I(2\omega) \propto \left| \mathbf{e}(2\omega) \cdot \chi^{(2)} : \mathbf{e}(\omega)\, \mathbf{e}(\omega) \right|^2 I(\omega)^2 \qquad (4)$$

where $\mathbf{e}(\omega)$ is the unit vector that describes the direction of the electric field of the fundamental beam, $\mathbf{e}(2\omega)$ is unit vectors that describes the direction of the electric field of the SH signal, $I(2\omega)$ is the intensity of the second harmonic light. Since $\chi^{(2)}$ is a vector, the product of $\mathbf{e}(2\omega)$ and $\chi^{(2)}$ is a vector, as is the product of $\mathbf{e}(\omega)$ and $\mathbf{e}(\omega)$. The ':' represents the inner product of these two vectors.

The nonlinear susceptibility is directly related to the average molecular orientation by this formula

$$\chi_{IJK}^{(2)} = N_S \Sigma < F > \beta_{ijk} \qquad (5)$$

where β_{ijk} is the microscopic nonlinear polarizability tensor element related to the SH response of an isolated molecule, N_S is the surface concentration of molecules, and <F> is the average orientation. [12] In chapter 4, β and <F> will be discussed in more detail in the context of organic adsorbates at the liquid - liquid interface.

$\chi_{IJK}^{(2)}$ is a tensor with twenty seven elements. Due to the geometry of our system, this tensor can be reduced to three unique components χ_{XXZ}, χ_{ZXX}, and χ_{ZZZ} [8] (see section 4.2.2 A ii) for more details). These three components of $\chi^{(2)}$ can be determined by varying the input polarization of the incident laser light and measuring the SH s- and p- polarized output. These curves can be fitted by the following equations, which are derived directly from equation (4),

$$I_s(2\omega) \propto | a_1 \chi_{XXZ} \sin 2\gamma |^2 I(\omega)^2 \qquad (6)$$

$$I_p(2\omega) \propto | (a_2 \chi_{XXZ} + a_3 \chi_{ZXX} + a_4 \chi_{ZZZ}) \cos^2\gamma + a_5 \chi_{ZXX} \sin^2\gamma |^2 I(\omega)^2 \qquad (7)$$

where $I_s(2\omega)$ represents the intensity of the s-polarized SH light, $I_p(2\omega)$ is the intensity of the p-polarized SHG, γ is the polarization angle of the incident light, $I(\omega)$ is the intensity of the input laser light and the a_i terms describe the electric fields in the monolayer. For our TIR experimental configuration, these constants are given by [24],

$$a_1 = \frac{64\pi(ik_o)n_1^2 \sin^2\theta \sin^2 67^o}{\left(n_2 \sin\theta + 2\sin 67^o\right)\left(\sin 67^o + n_1 \sin\theta\right)^2 \left(1+n_1\right)^2}$$

$$a_2 = \frac{64\pi(\ ik_o\ )n_1^5 n_2 \cos 67^o \sin^2\theta \sin^2 67^o}{\left(\sin 67^o + 2n_2^3 \sin 67^o\right)\left(\sin 67^o + n_1 \sin\theta\right)^2 \left(1+n_1\right)^2}$$

$$a_3 = \frac{64\pi(\ ik_o\ )n_1^7 n_2 \cos^3 67^o \sin^2 67^o}{\left(\sin 67^o + 2n_2^3 \sin 67^o\right)\left(\sin 67^o + n_1 \sin\theta\right)^2 \left(1+n_1\right)^2} \qquad (8)$$

$$a_4 = \frac{256\pi(\ ik_o\ )n_1 3n_2 \cos 67^o \sin^2 67^o}{\left(\sin\theta + 2n_2^3 \sin 67^o\right)\left(n_1 \sin 67^o + \sin\theta\right)^2 \left(1+n_1\right)^2}$$

$$a_5 = \frac{256\pi(\ ik_o\ )n_1 4\cos 67^o \sin^2 67^o}{\left(n_1 \sin\theta + \sin 67^o\right)\left(n_1 \sin 67^o + \sin\theta\right)^2 \left(1+n_1\right)^2 \left(\sin 67^o + 2n_2 \cos 67^o\right)}$$

where k_o is the wave vector of the fundamental wave, n_1 is the refractive index of the water, n_2 is the relative refraction index of the carbon tetrachloride at the second harmonic wavelength and θ is as shown in figure 3.1.

By fitting the experimental curves with equations (6) and (7) the components of $\chi^{(2)}$ can be determined.

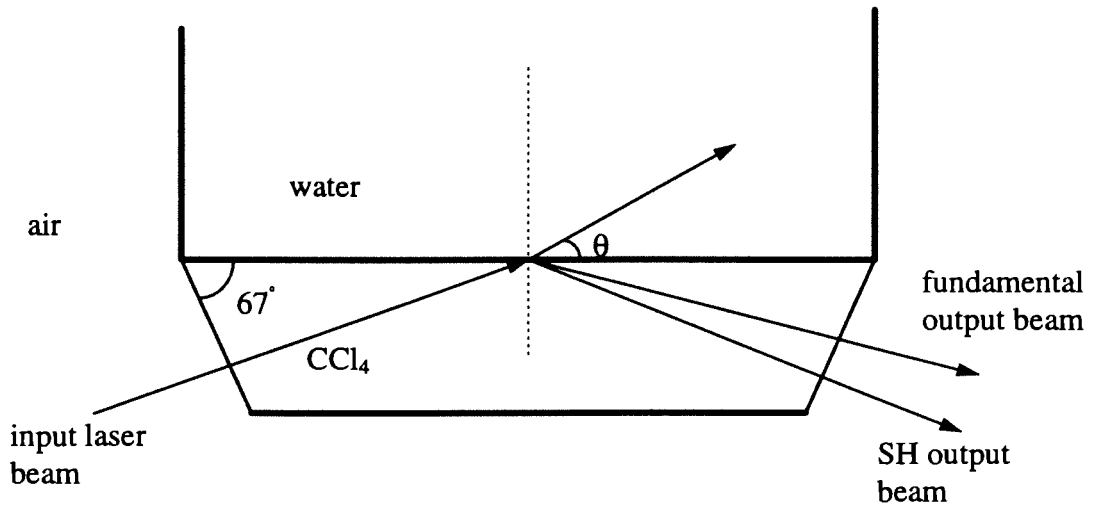

Figure 3.1: Schematic representation of the interface

3.4) Results and Discussion

The signal that is obtained from the neat water / CCl_4 interface arises from the broken symmetry at the interface and from the nonlinear polarizability of the water molecule present there. Shown in figure 3.2 is the polarization dependence curve for the water molecules at the water / CCl_4 interface. The

polarization of the incident light is varied and plotted against the second harmonic signal intensity. The solid circles represent the p-polarized light while the empty circles represent the s-polarized light. The lines represent the theoretical fits based on the calculations of the previous section. The error in these points is less than ten percent in the y direction and two degrees or less in the x direction. These uncertainties were determined by reproducing the signal at particular polarization angles several times and determining the standard deviation.

It should be noted that even though the data is of reasonable quality, the signal generated from the water molecules at the neat water / CCl_4 interface is very small compared with signals generated from other interfaces that have a similar interfacial concentrations, such as p-nitroaniline at the water / CCl_4 interface (see section 4.2).

We also have determined through our experiments that the polarization curve characteristic of an interface free of contaminants is like the one shown in figure 3.2. When organic species or other contaminants are at the interface, the phase of the polarization curve is shifted and the appearance of the curve is considerably different (for an example see figure 4.4). Thus we can use the phase of the curve as a sign for a clean interface.

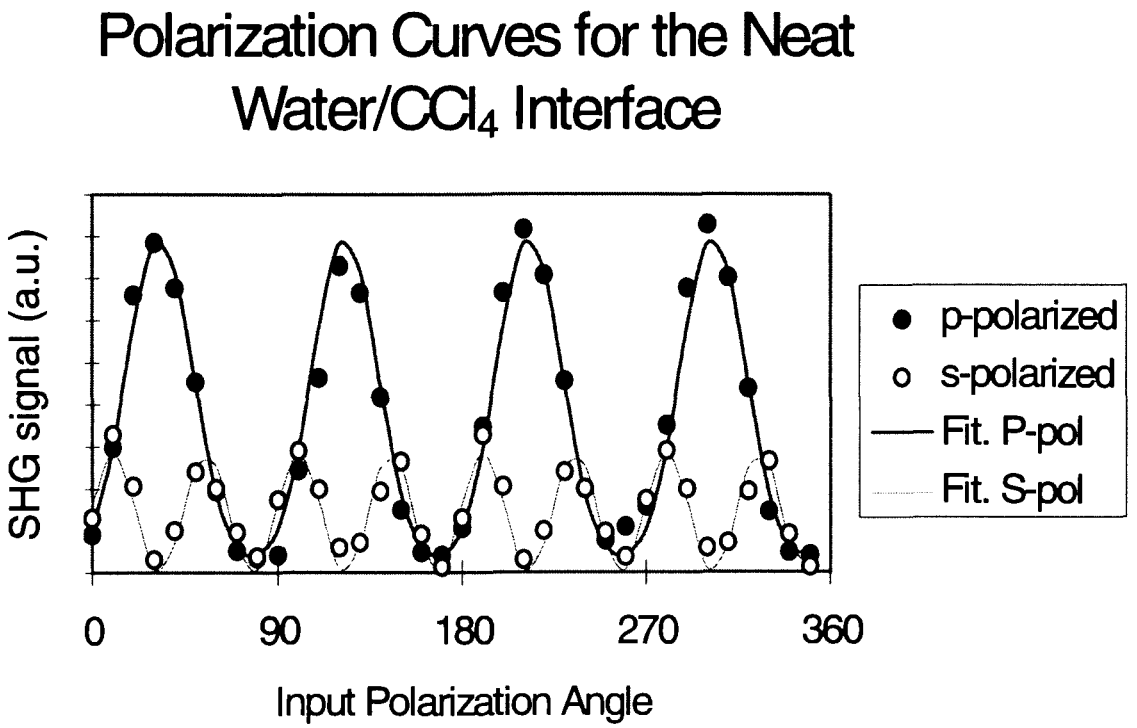

Figure 3.2) Orientation curves of s-and p- polarized SH signal for the neat water /CCl_4 interface, where filled in circles represent p-polarized and hollow circles represent s-polarized. Lines represent theoretical fits.

The s-polarized signal is fitted first because it only has one χ parameter in the formula for the fitting (see equation 6). This χ parameter, χ_{xxz}, is extracted from fitting the experimental data with this equation. Then we fix this parameter and vary χ_{zzz} and χ_{zxx}, using equation (7) to fit the p-polarized curve. It should

also be noted that the s-polarized curve has twice the periodicity of the p-polarized curve (see equations 6 and 7). Looking at figure 3.2, one can verify that this is the case for our experimental data, indicating that it is in fact a second harmonic generated signal.

From the theoretical fitting procedure, we extract the χ values. For the water molecules at the interface, χ_{zzz} was found to be negligible, while the ratio of the other components was found to be $\chi_{xxz} : \chi_{zxx}$ of $1 \pm 0.08 : -1.50 \pm 0.09$. The error on these susceptibilities was determined as explained in section 4.2.2B.

Using the following relationship

$$\chi_{zzz} + \chi_{xxz} + \chi_{zxx} = N_s (\alpha + \beta) < \cos\theta > \qquad (9)$$

where N_S is the number of surface molecules, θ is the angle between the dipole and the surface normal, and α and β are hyperpolarizability components, we can deduce the value of θ.[19] Our results yield a very small number on the left hand side of the equation. Since $(\alpha+\beta)$ is a nonzero number[25], our results would yield a very small number equal to the cosine θ.

At the water / CCl_4 interface there are a large number of water molecules, even so the SH signal is small. There are two possible reasons for this small signal. One possible reason for the small SH signals observed in these experiments is that there may be a broad distribution of orientations of water molecules at the interface. This would argue in favor of a small energy barrier to molecular reorientation. Since two water molecules having opposite orientations

would cancel their contribution to χ, a broad distribution of the orientation would tend to have a signal canceling effect with the result that the SH signal would be reduced. A second possible explanation for the small SH signals is that the water molecules have a narrow distribution of orientations. In this case from equation (9), $< \cos \theta > \approx \cos <\theta>$ which is a very small number, thus theta is approximately 90°. That would mean that the structure at the interface is such that the dipoles of the water molecules are close to parallel to the interface. This situation would be expected to yield a small SH signal. A schematic representation of this is given in figure 3.3. Of course, it is impossible for all of the water molecules to have such an orientation and still maintain an energetically favorable hydrogen bonded network. Thus other water molecules must be oriented such that their contributions to the SH signal cancel each other. This would also account for the small signal.

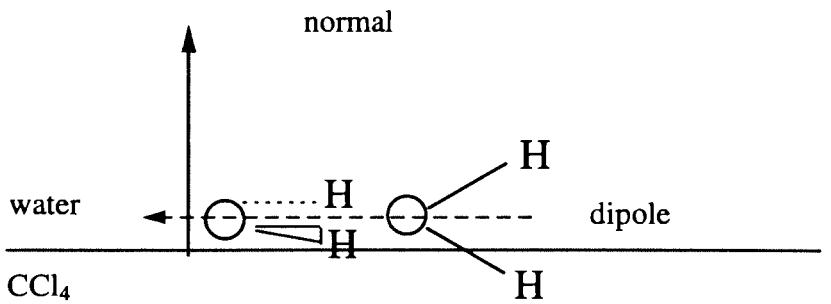

Figure 3.3 : Schematic representation of one possible orientation of a water molecule at the water / CCl_4 interface.

Y.R. Shen *et. al.*[26, 27] have reported surface vibrational spectroscopy studies at three different water / hydrophobic interfaces; water / air, water / surfactant covered quartz, and water / hexane. They have determined that 25 % of the water molecules in a full monolayer have one of their hydrogen atoms pointing toward the non-polar phase. Our results are consistent with this view. With the water molecules unable to participate in any hydrogen bonding they are aligned with their dipoles parallel to the interface and some of the hydrogens are pointing toward the CCl_4 phase. These hydrogens would give rise to a large surface vibrational spectrum. Since the dipoles are close to parallel to the interface, the SH signal is small but as expected a fairly large surface vibrational signal could be obtained with a frequency shifted peak for the OH's that are pointed out of the water, which is what Shen observed.

Chapter 4: Investigation of p-Nitroaniline and its pH Dependence at the Water / Carbon Tetrachloride Interface

4.1) Introduction

The behavior of organic molecules at interfaces has been the subject of intense study for almost a century. [1] Despite the widespread interest in this field, an investigation of these interfaces on a molecular level remains an experimental challenge. As mentioned in section 1.1, molecules at a liquid - liquid interface are especially difficult to investigate due to contributions in signal from the large number of solute molecules in the bulk. The surface specific non-linear optical technique, second harmonic generation, conquers this problem. Second harmonic generation (SHG) is forbidden in the bulk media, thus it may be used as a probe for molecules at the liquid - liquid interface.

P-nitroaniline was chosen as a probe molecule to investigate the adsorption energetics and orientation effects at the water / CCl_4 interface because of its large nonlinear response. This large response is a result of the strength of the pNA donor and acceptor groups on opposite ends of the molecule. This leads to a large nonlinear polarizability, β (refer to section 1.2 for more details).

This investigation employs SHG as a spectroscopic tool in the detection of monolayer and submonolayer coverages of p-nitroaniline at the water / CCl_4 interface. We have used this technique to determine the Gibbs free energy of adsorption ($\Delta G°_{ads}$) of pNA, and to determine its averaged molecular orientation. As well, the molecular orientation and SH signal intensity were investigated at this interface as a function of solution acidity to monitor the adsorption energetics of an organic ion at this liquid - liquid interface. These results provide an example of interfacial chemical equilibrium and allow one to contrast aspects of this equilibrium with those observed in the bulk phase.

In section 4.2 and section 4.3, descriptions of the adsorption energetics and averaged molecular orientation of pNA and the protonated pNA at the water / CCl_4 interface are presented.

4.2) Second Harmonic Generation Studies of P-nitroaniline at the Water / CCl_4 Interface

4.2.1) Chemical Equilibrium: The Adsorption Isotherm

Recalling equation (4), the intensity of the second harmonic light is proportional to the susceptibility squared multiplied by the intensity of the input light squared (see equation 10).

$$I(2\omega) \propto (\chi^{(2)})^2 (I(\omega))^2 \qquad (10)$$

As will be discussed later in section 4.2.2 A), the $\chi^{(2)}$ is proportional to the number of molecules at the interface. So the SH signal generated is proportional to the number of molecules squared. Thus a plot of the square root of the SH intensity versus the concentration of the molecules in the bulk yields an adsorption isotherm which is a measure of the number of interfacial molecules which undergo adsorption. The experimental setup is described in detail in section 2.2.2).

4.2.1 A) The Langmuir Isotherm

The relationship between the amount of substance adsorbed at the interface and a physical property of the interface (like the surface tension or the second harmonic signal generated there) at a given temperature, is called an adsorption isotherm. The Langmuir isotherm is the simplest isotherm and is based on three assumptions.[28] The first is that maximum coverage is a monolayer, thus no adsorption occurs beyond this. The second assumption is that all sites available for adsorption are equivalent and the surface is uniform. The final assumption is that the molecule's ability to be adsorbed is independent of the occupation of neighboring sites.

There is an adsorption and desorption equilibrium that exists between the bulk pNA molecules (M) and the free surface sites (S), giving rise to filled surface sites (MS), represented by the following equation [15]

$$M + S \underset{k_2}{\overset{k_1}{\rightleftharpoons}} MS \qquad (11)$$

where k_1 is the rate constant for adsorption in molecules per second and k_2 is the rate constant for desorption. The kinetic equation [15] is

$$\frac{dN}{dt} = k_1 \frac{C}{555}(N_{max} - N) - k_2 N \qquad (12)$$

where N is the number of adsorbed molecules, N_{max} is the maximum number of adsorbed molecules, C is the concentration of the bulk in moles/ liter, and 55.5 is the molarity of water. The first term in this equation describes the rate of adsorption and the second term describes the rate of desorption. At equilibrium dN/dt = 0 and

$$\frac{1}{N} = \left(\frac{55.5 \frac{k_2}{k_1}}{N_{max}} \right) \frac{1}{C} + \frac{1}{N_{max}} \qquad (13)$$

Since 1/N is proportional to the inverse of the square root of the SH intensity, a plot of the inverse of the square root of the SH intensity versus the inverse bulk concentration will yield a straight line with intercept equal to the inverse of the maximum number of adsorbed molecules possible, and slope of $(55.5/N_{max})(k_1/k_2)$, where

$$\frac{k_2}{k_1} = \exp\left(\frac{\Delta G^{o}_{ads}}{RT}\right) \tag{14}$$

and $\Delta G°_{ads}$ is the free energy of adsorption and T is the temperature in degrees Kelvin.

The kinetic equation at equilibrium can also be rewritten in the more common Langmuir adsorption equation [15]

$$\frac{N}{N_{\max}} = \frac{C}{C + \left(55.5\frac{k_1}{k_2}\right)} \tag{15}$$

This equation can be used directly in a theoretical fit to the plot of square root of intensity versus concentration.

4.2.1 B) Results and Discussion

Figure 4.1 shows the adsorption isotherm obtained for pNA at the water/ CCl_4 interface. The curve starts at the background level which is essentially the signal generated from the clean water / CCl_4 interface. As the bulk concentration increases, the signal increases until a monolayer is formed at which point the curve levels off. Higher concentrations could not be investigated since pNA is not extremely soluble in water. In figure 4.1, the squares represent

experimental data. The best fit was attained by a nonlinear least squares fit to equation 13 as will be discussed below. The error bars were determined by repeating various concentrations and observing the variation in signal. At low concentrations the error was approximately twenty percent of the square root of the intensity and at high concentrations the error was approximately five percent.

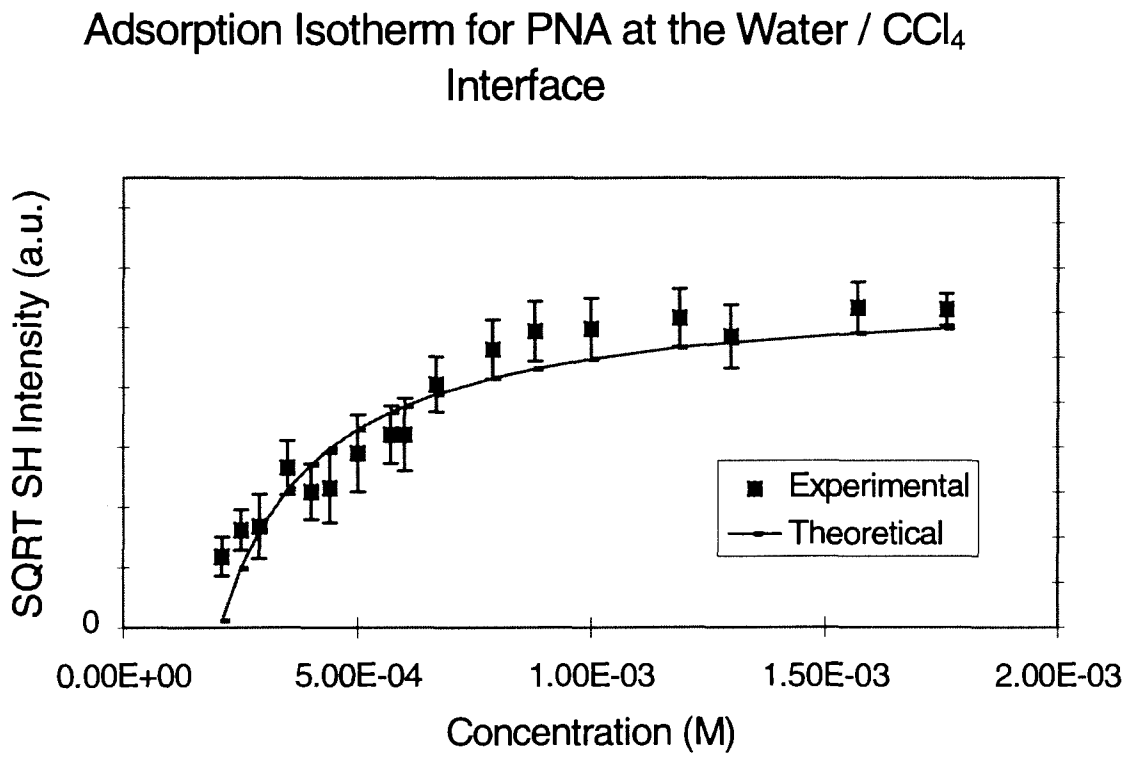

Figure 4.1 : A plot of the square root of the SH intensity versus bulk concentration for pNA. The squares represent experimental results and the line is the theoretical fit, based on the Langmuir isotherm.

A nonlinear least squares fit to equation 13 yields a straight line as can be seen in figure 4.2. Since the square root of the SH intensity is proportional to the number of adsorbed molecules, according to equation 13 a plot of the inverse of the SH signal versus the inverse of the bulk concentration will yield a straight line. The squares represent the experimental results and the line is a best fit. The slope of this line is 7.93×10^{-4} M and the intercept is equal to 7.56×10^{-2}. The value of k_1/k_2 was calculated to be 1.13×10^{-7}. The error is greater at the lower concentration, as previously discussed in this section and was determined by repeating various concentrations and determining the standard deviation. Using these values and equations 13 and 14, the Gibbs free energy of adsorption was determined to be -9.48 ± 0.37 kcal/mol.

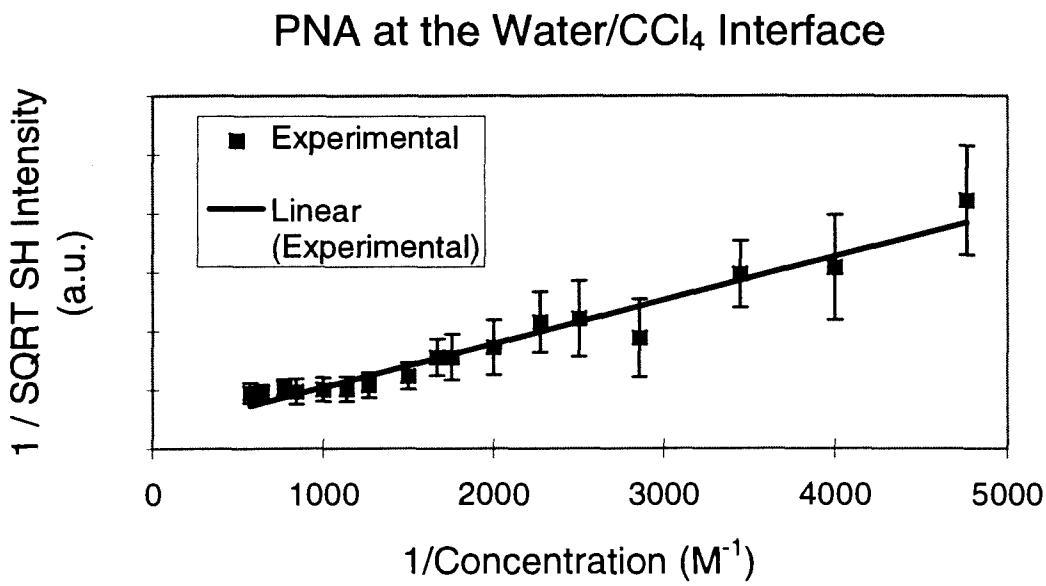

Figure 4.2 : A plot of the inverse of the square root of the SH signal versus the inverse of the bulk concentration of pNA. The squares represent experimental results and the line is the theoretical fit.

Similar studies have previously been performed and some discussion of these is necessary to put their results into context. An investigation by Higgens *et. al.*[8] determined that the nitro group in p-nitrophenol is directed away from water at the water / air interface. Using chemical intuition in the case of pNA, it would be reasonable to assume that the NO_2 group is the non - polar group and is pointed toward the CCl_4. The NH_2 group is more polar and also can form hydrogen bonds with water molecules in the the aqueous phase. Using SHG, Castro *et. al.*[15] have examined the behavior of p - *n* - alkylanilines with zero to six and ten carbons in the hydrocarbon chain at the air / water interface. These molecules are amphiphilic, meaning they have both hydrophilic and hydrophobic components.[23] The molecules were oriented with their hydrophobic chain pointed out of the water and the hydrophilic -NH_2 group in the water phase. They found a linear relationship between carbon chain length and $\Delta G°_{ads}$ where the $\Delta G°_{ads}$ changed by 0.78 kcal/mol with every additional CH_2 unit in the alkyl chain. It was concluded that the free energies of adsorption became more negative (from -3.5 to -11.3) with increasing chain length. This is consistent with the fact that hydrophobicity increases with chain length. Thus the molecules would prefer to be adsorbed at the interface where the hydrophobic chain can be away from the water and the hydrophilic group can be in the water. Comparison our results to Castro *et. al.*[15] would indicate that the nitrobenzene portion of the molecule behaves in the same manner as an alkyl benzene with chain length between five and eight carbons, implying a large hydrophobic interaction. However, our interface and those studied by Castro [15], although they have

similar properties, are not the same. Therefore to make a more direct comparison, a future study would need to investigate other anilines at the water / CCl_4 interface to see if similar behavior is observed.

4.2.2) Polarization Studies

The averaged molecular orientation of p-nitroaniline at various concentrations was determined by a method that is outlined in section 4.2.2 A). The experimental procedure is as described in section 3.2 and chapter 2.

4.2.2 A) Determination of the Interface Susceptibilities

The interface susceptibility, $\chi^{(2)}$, is directly related to the averaged molecular orientation by the following formula:

$$\chi_{IJK}^{(2)} = N_S \Sigma \langle F_{IJKijk}(\varepsilon, \theta, \alpha) \rangle \beta_{ijk} \qquad (16)$$

where β_{ijk} is the nonlinear polarizability tensor element related to the SHG response of an isolated molecule, N_S is the surface concentration of molecules, and $\langle F_{IJKijk}(\varepsilon, \theta, \alpha) \rangle$ describes the averaged molecular orientation. The angles ε, θ, and α are described in figure 4.3.

To determine the averaged molecular orientation, one must first determine what parameters of β are important and how to obtain values for them through calculation or chemical intuition. Once the β_{ijk} elements are defined, and

$\chi^{(2)}_{IJK}$ determined experimentally, they can be related in order to extract the molecular averaged orientation, <F>.

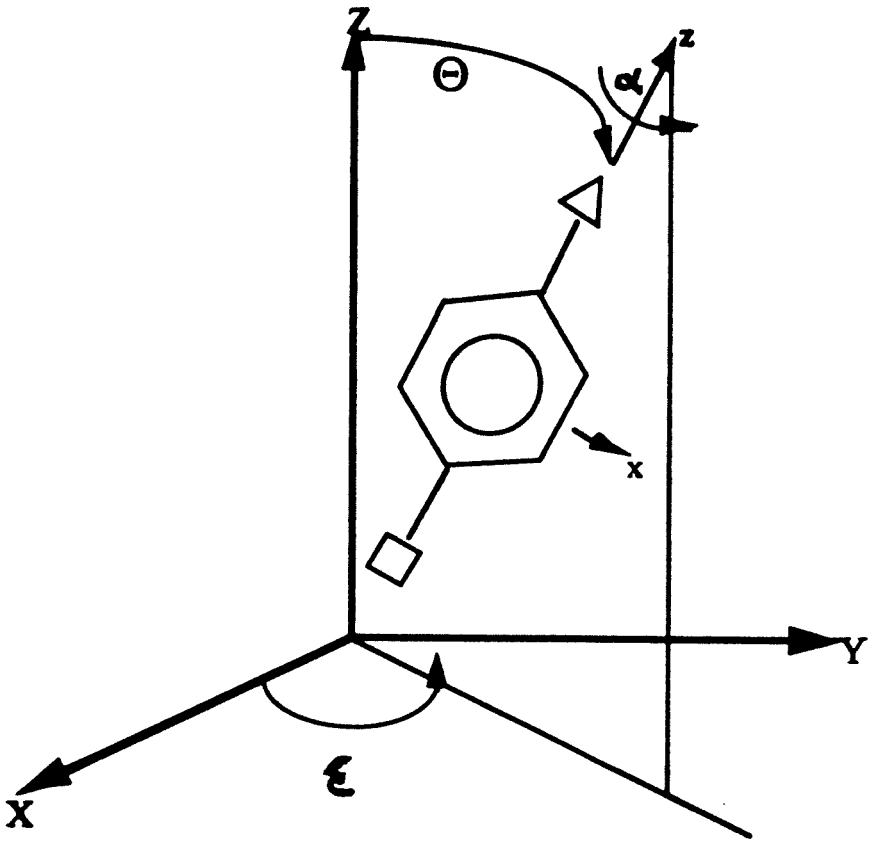

Figure 4.3 : Definition of ε, θ, and α. The surface normal is the Z axis. The triangle and square represent the NH_2 and NO_2 groups. [2]

i) Molecular Nonlinear Polarizabilities

Assuming a simple two level model where one only considers a ground state and a single excited state, the equation for the elements of the nonlinear polarizability tensor are given by [12]

$$\beta_{ijk} = \frac{-e^3}{2h^2}\left[\frac{\Delta r_n^j r_{ng}^{\ i} r_{ng}^{\ k}}{\omega_{ng}^2 - \omega^2} + r_{ng}^i (r_{ng}^j \Delta r_n^k + \Delta r_n^j r_{ng}^k)\frac{(\omega_{ng}^2 + 2\omega^2)}{(\omega_{ng}^2 - 4\omega^2)(\omega_{ng}^2 - \omega^2)}\right] \qquad (17)$$

where Δr_n is the difference in permanent dipole moment between excited state *n* and ground state *g*, r^i_{ng} is the transition dipole matrix element between states *n* and *g* along the molecular axis *j*, ω is the incident laser frequency, and ω_{ng} is the difference in frequency between the ground and excited states. When the frequency of the energy level ω_{ng} is close to or resonant with the frequency of the laser light, ω, or the second harmonic light, 2ω, then the β's increase dramatically thus the $\chi^{(2)}$'s increase and in turn the SHG is much enhanced. [6] In cases where r_{ng} and Δr_n are collinear, the polarizability tensor is simplified dramatically and only β_{zzz} is nonzero. In more complicated cases such as this one with many real energy levels, working with only one tensor element is an oversimplification, and other contributions cannot be neglected. [29] For molecules

such as p-nitroaniline calculations have been completed [29] to determine that only two components β dominate: β_{zzz} and β_{zxx}.

ii) Surface Nonlinear Susceptibility

$\chi_{IJK}^{(2)}$ is a tensor element with twenty seven elements. This tensor can be reduced by assuming that the molecules at the interface are randomly oriented in terms of rotation around the surface normal, Z. That is to say that a random distribution of ε is assumed. For example, χ_{xxy} will be zero following this assumption. The polarization in this case is

$$P_X = \chi_{XXY} E_X E_Y \qquad (18)$$

where E is the electric field intensity. Assuming that we can rotate it around the Z axis, then

$$\chi_{XXY}\, E_X E_Y = \chi_{XXY}\, (-E_X)(-E_Y)$$

so,

$$P_X = -P_X$$

which is only true when the χ_{XXY} term is zero. Similarly twenty four of the twenty seven components of χ_{IJK} are zero, leaving only three nonzero components of $\chi^{(2)}$ which are χ_{xxz}, χ_{zxx}, and χ_{zzz}. As described in detail in section 3.3 these components of $\chi^{(2)}$ can be determined by varying the input polarization of the incident laser light and measuring the SHG output at 0° with respect to the plane

of incidence of the sample (s-polarized) and at 90° with respect to the plane of incidence (p-polarized). These curves can be fitted by the following equations,

$$I_s(2\omega) \propto | a_1 \chi_{XXZ} \sin 2\gamma |^2 I(\omega)^2 \quad (6)$$

$$I_p(2\omega) \propto | (a_2 \chi_{XXZ} + a_3 \chi_{ZXX} + a_4 \chi_{ZZZ}) \cos^2\gamma + a_5 \chi_{ZXX} \sin^2\gamma |^2 I(\omega)^2 \quad (7)$$

iii) Molecular Orientation Determination

In this case, when only two components of β are dominant, the relative magnitudes of β_{ZZZ} and β_{ZXX} can be obtained from the experimentally determined values of the $\chi^{(2)}$ elements as shown in equation (19).[29]

$$\frac{\beta_{ZXX}}{\beta_{ZZZ}} = 2\frac{\chi_{ZXX} - \chi_{XXZ}}{\chi_{ZZZ} + 2\chi_{XXZ}} \quad (19)$$

As well, an orientation parameter D can be defined such that[29]

$$D = \frac{\langle \cos^3\theta \rangle}{\langle \cos\theta \rangle} = \frac{\chi_{ZZZ} - \chi_{ZXX} + \chi_{XXZ}}{\chi_{ZZZ} + 3\chi_{XXZ} - \chi_{ZXX}} \quad (20)$$

Assuming the distribution of θ is narrow, $\langle \cos^3\theta \rangle \approx \cos^3\langle\theta\rangle$ and $\langle \cos\theta \rangle \approx \cos\langle\theta\rangle$. From this, the average angle of the molecule with respect to the surface normal, $\langle\theta\rangle$, can be determined.

4.2.2 B) Results and Discussion

The orientation curves for the s- and p- polarized light, for pNA with bulk concentration of 5.5 x 10^{-4} M, are shown in figure 4.4. The polarization of the incident light is plotted against the second harmonic signal intensity. The solid circles represent the p-polarized SH signal and the empty circles represent the s-polarized SH signal. The lines represent theoretical fits based on the calculations described in the previous section. The error in these points is less than ten percent in the y direction and two degrees or less in the x direction, and was determined by repeat trials. The curves are fitted by fitting the s-polarized curve first and determining χ_{xxz}. Then χ_{xxz} is fixed while the p-polarized curve is fitted and the other two χ's are extracted.

When the experimental data for the orientation was fit theoretically for the neutral p-nitroaniline, the ratio of $\chi_{xxz} : \chi_{zxx} : \chi_{zzz}$ was found to be $1.00 \pm 0.16 : 1.12 \pm 0.16 : 1.85 \pm 0.21$, and the ratio of $\beta_{zxx}/\beta_{zzz} = 0.017 \pm 0.011$. The error for in these values was determined as follows. Here is a typical value for pNA at a concentration of 5.5 x 10^{-4} M.

$$\chi_{xxz} = 0.725 \pm 0.059$$

$$\chi_{zxx} = 0.750 \pm 0.051$$

$$\chi_{zzz} = 1.328 \pm 0.042$$

The errors were extracted by nonlinear least squares fitting of the polarization curves. The ratio of these values was calculated to be $\chi_{xxz} : \chi_{zxx} :$

χ_{zzz} = 1.00 ± 0.16 : 1.03 ± 0.16 : 1.83 ± 0.21. All curves demonstrated approximately the same error so this error was taken to be representative of all the pNA curves. All the errors in the χ ratios throughout this paper have been determined in this manner. From these χ's, the averaged orientation angle with respect to the surface normal, θ, was calculated to be 48° ± 0.05°. This is comparable with results reported for p-nitrophenol at the air / water interface where a value of 55° was obtained. [11-13] The θ remained constant over all concentrations, indicating that the averaged orientation did not vary with concentration. It should be noted that the angles determined by these SHG experiments reflect an averaged orientation angle and do not reflect molecular tumbling of interfacial molecules. SHG is a coherent scattering parametric process and in this experiment induced by laser pulses of 100 fs, much shorter than rotional periods of molecules, which are typically more than 1 ns. In other spectroscopies (for example, polarized fluorescence, NMR) special techniques such as magic angle spinning are used in the detection of 'excited' molecules (i.e. adsorption has already selected a subset of species being probed) in order to remove the geometric contribution to the signal.[32] Thus, SHG serves as a probe of interfacial averaged molecular orientation.

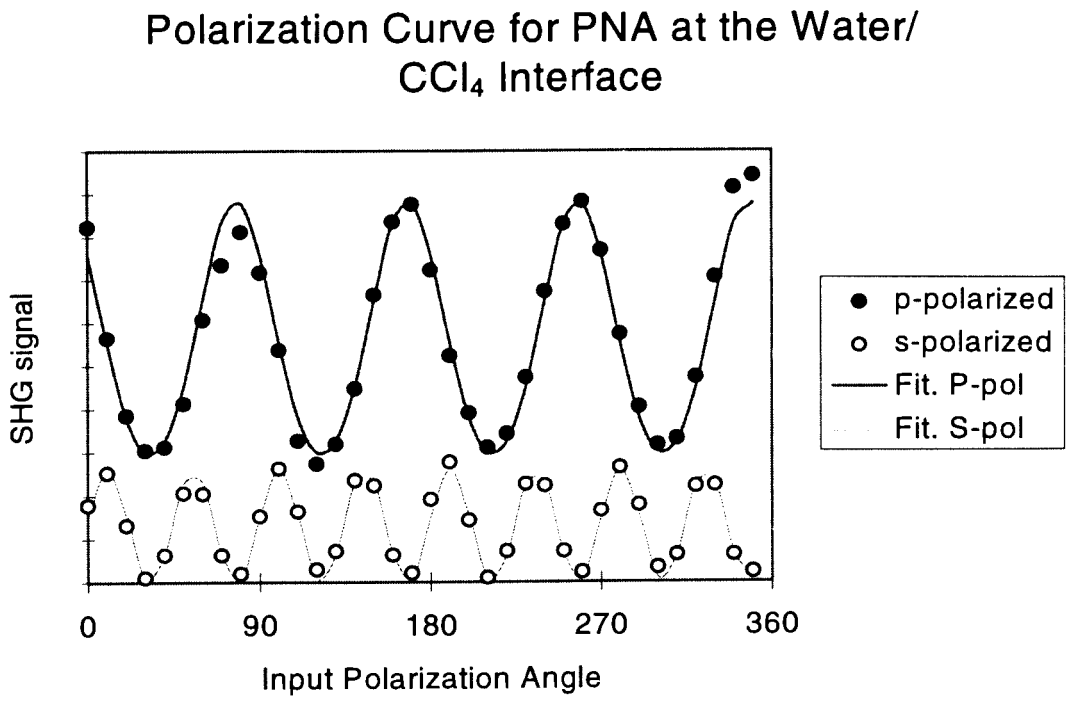

Figure 4.4 : Polarization curves for pNA at a concentration of 5.5 x 10^{-4} M. Filled circles represent experimental data for the p-polarized signal. Open circles represent experimental data for the s-polarized SH signal. Lines represent theoretical fits as described in section 4.2.2 A.

4.3) Investigation of the pH Dependence of p-Nitroaniline

4.3.1) Adsorption Isotherm

4.3.1 A) SH Signal Dependence on pH

The acidity of pNA was varied by additions of 0.007M hydrochloric acid (HCl) and 0.007M sodium hydroxide (NaOH) to a 5.5 x 10^{-4} M solution of pNA at the interface, which corresponds to a surface coverage of approximately eighty percent. The SH signal increases with the addition of acid but does not change significantly upon addition of base (see figure 4.6. Stizman [9] investigated the effect that increasing the chain length (n) of p-n-anilinium ions had on the SH signal. They found that chain lengths shorter than four carbons showed no SH signal generated at the interface due to the strong solvation in the bulk phase, but that the signal increased linearly with increasing carbon chain length after four carbons. When there are more than four carbons in the chain, the hydrophobicity overcomes this solvation. Thus our results imply that the hydrophobic interaction of NO_2, acting in a similar manner as long chain hydrocarbons, drives more cations to the interface, thus increasing the signal. The increase in signal with the addition of acid is consistent with the assertation that the NH_2 group of the pNA is pointed up into the water as we have argued previously. Upon addition of acid interfacial pNA molecule can become protonated (see fig. 4.5). One might expect the signal to vanish as a result of

the ions moving away from the interface into the water to be solvated, but this is not the case.

The reason the signal increases is because this protonation creates a large dipole within the molecule which increases the $\chi^{(2)}$, which in turn increases the SH signal intensity since the $(\chi^{(2)})^2$ is proportional to the signal intensity.

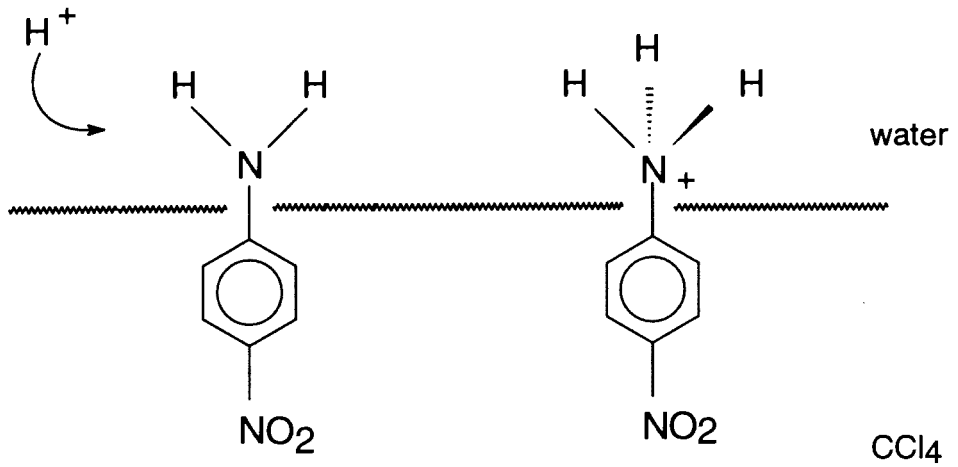

Figure 4.5 : Schematic representation of the protonation of p-nitroaniline at the water / CCl_4 interface.

Figure 4.6 shows the pH dependence of the SH signal of pNA at the water / CCl_4 interface. As can be seen there is a large increase in signal with decrease in pH. The error bars were determined by repeated trials at various pH's.

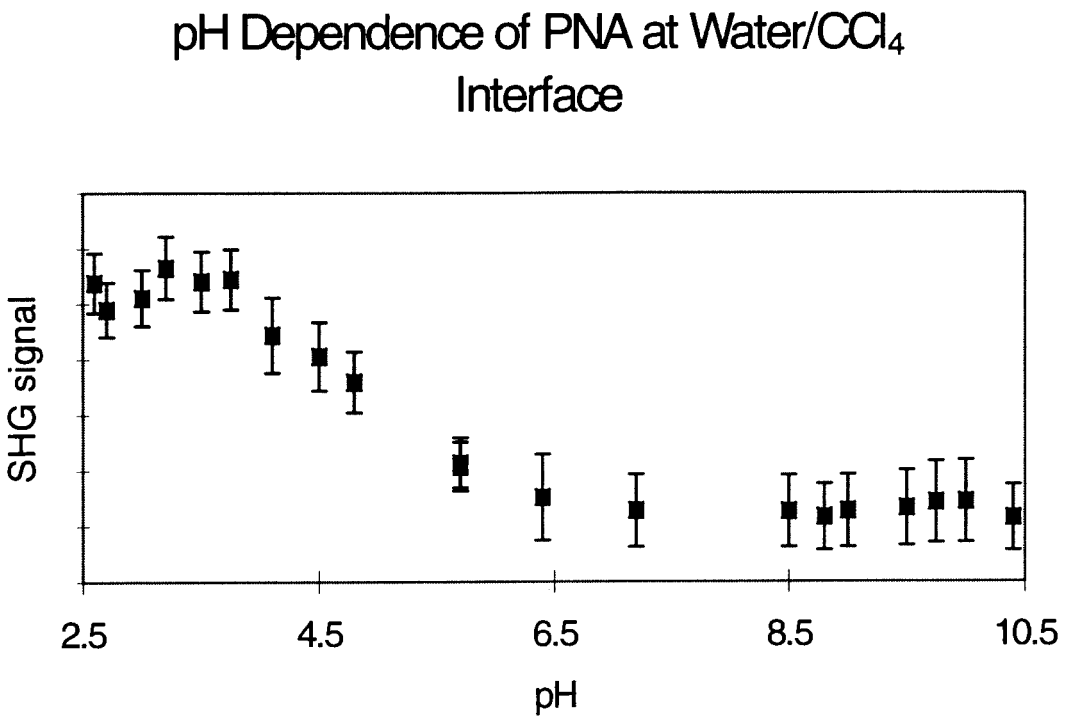

Figure 4.6 : Plot of second harmonic signal intensity versus pH.

The adsorption isotherm for the concentration of pNA cations has been theoretically fit and a $\Delta G°_{ads}$ was determined and will be discussed in the next section.

4.3.1 B) Adsorption Isotherm : Results and Discussion

Figure 4.7 is a plot of the inverse SH signal versus the inverse concentration at pH = 3.5. The pKa of pNA in bulk solution is 1.0. The percent dissociation at this pH is 99.7%, meaning that the vast majority of pNA in solution exists in ionic form. The squares represent the experimental data and the lines represent the theoretical data based on the Langmuir isotherm. This plot yields a straight line as would be expected from equation 13.

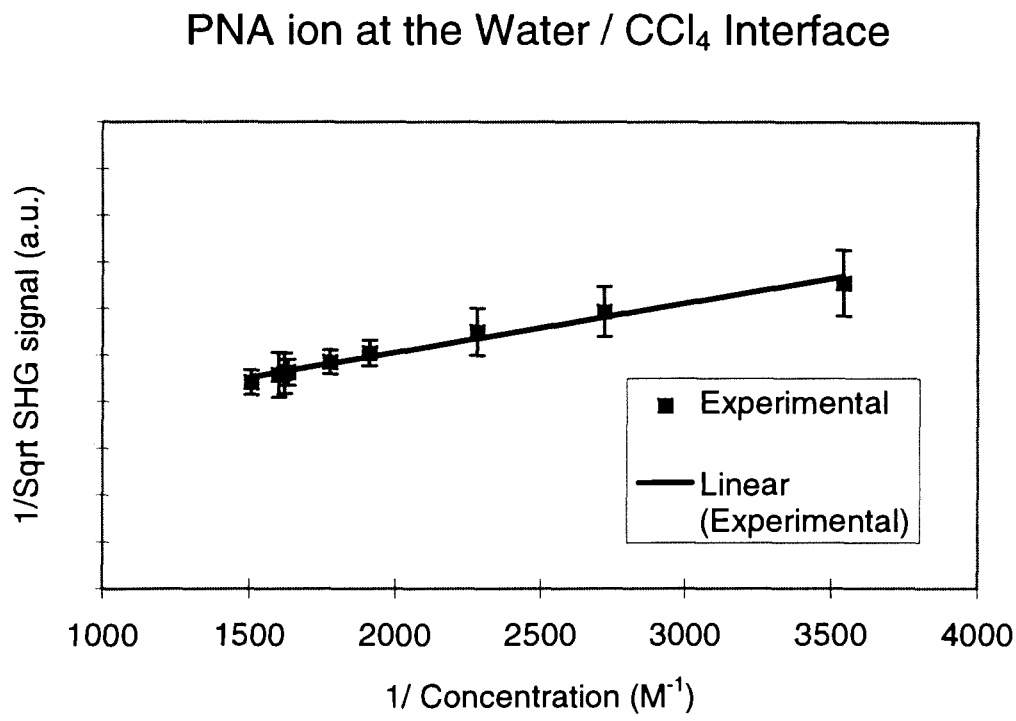

Figure 4.7 : A plot of the inverse of the SH signal versus the inverse of the bulk concentration of pNA ions. The squares represent experimental results and the line is the theoretical fit based on the Langmuir isotherm.

The adsorption isotherm of the protonated pNA molecule was fit theoretically in the manner described in section 4.2.1 A. Although the Langmuir model assumes no interaction between the molecules and even though these are ions that may repel each other, the Langmuir isotherm provides a good fit to the data. Interestingly the model is successful, implying that the amphiphilic nature of the molecule dominates over the repulsive effects or that the steric effects of the organic molecule keep the charges far enough away from each other so that the ionic replusions do not effect the signal.

Fitting the experimental data with equation 13 gives a slope of 5.25×10^{-5} M and an intercept of 0.346, as seen in figure 4.7. This corresponds to a $\Delta G°_{ads}$ of -7.75 kcal/mol $\pm$ 0.26 kcal/mol. This is in line with the work of Castro *et. al.*[15] who noted a decrease in the magnitude of $\Delta G°_{ads}$ relative to the neutral molecule. It is likely that this decrease is a result of the extra work involved in removing the ions from a solvated state in the water and bringing them to the interface and due to the extra work involved in bringing an ion to an already charged interface.

One can estimate the magnitude of these electrostatic effects by dividing the observed $\Delta G°_{ads}$ into amphiphile and electrostatic contributions: [15]

$$\Delta G°_{ads} = \Delta G°_{ads}{}^{amp} + \Delta G°_{ads}{}^{ion} \qquad (21)$$

where $\Delta G°_{ads}{}^{amp}$ is that of the amphiphile and can be estimated to be the $\Delta G°_{ads}$ observed for the neutral pNA molecule (section 4.2.1 B), and $\Delta G°_{ads}{}^{ion}$ is that of the electrostatic contribution. Comparison of the values of $\Delta G°_{ads}$ obtained for

the pNA and the p-nitroanilinium results in an electrostatic contribution of 1.73 kcal/mol.

4.3.2) Polarization Studies

The polarization curve for the pNA ion at various pH's were obtained and fitted with the method outlined in section 4.2.2.

4.3.2 A) Results and Discussion

Figure 4.8 shows an s- and p- polarization curve for pNA at a pH of 3.5. Again, the filled circles represent the p-polarized signal and the empty circles represent the s-polarized signal. The lines represent the theoretical best fits determined as described in 4.2.2 A. The θ values do not change with increased ion concentration, in fact they are the same as the neutral pNA, $47.0° \pm 0.08°$ hence, the forces holding these molecules at the interface are dominant over the ionic repulsion forces. The pNA cations' orientation measurements gave a ratio of $\chi_{xxz} : \chi_{zxx} : \chi_{zzz}$ of $1.0 \pm 0.13 : 1.3 \pm 0.14 : 1.9 \pm 0.18$. The errors were determined in the same manner as those for the neutral pNA molecule (see section 4.2.2 B). The difference from that of the neutral pNA χ ratio arises from the increased polarization of the interfacial molecules due to protonation.

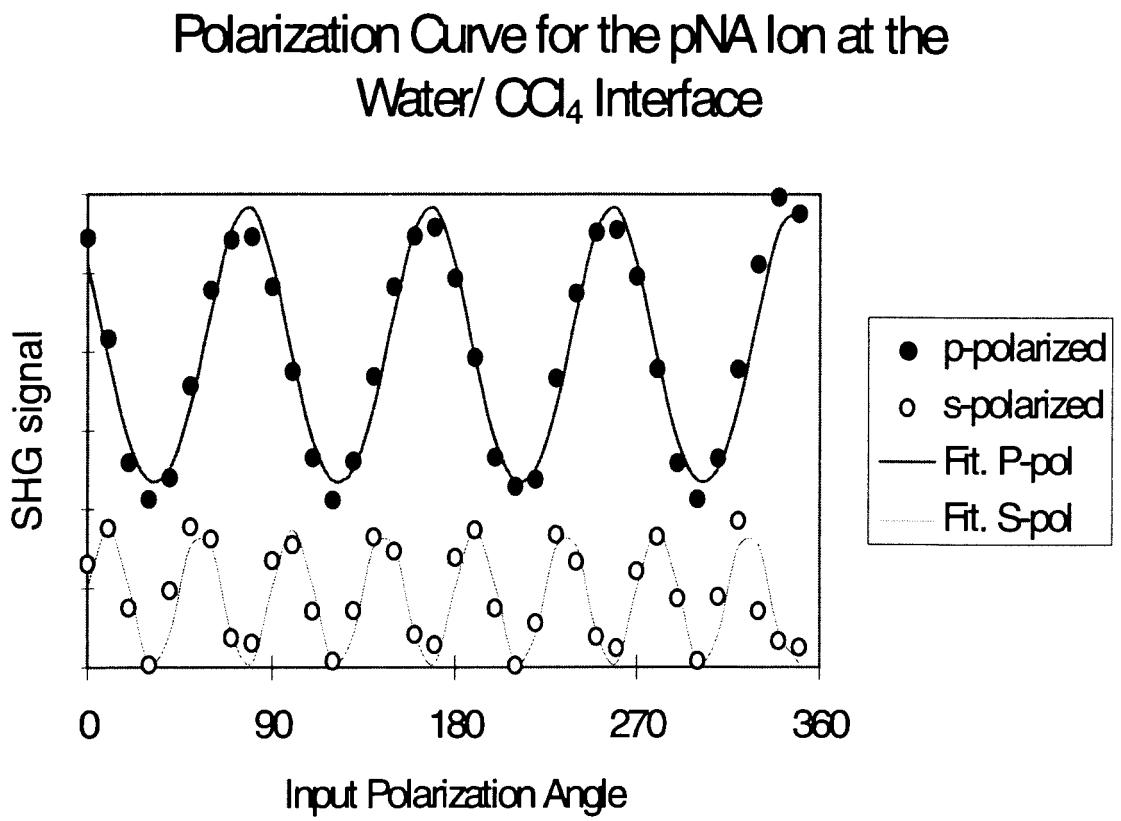

Figure 4.8 : Polarization curves for pNA at pH = 3.5. Filled circles represent experimental data for the p-polarized signal. Open circles represent experimental data for the s-polarized SH signal. Lines represent theoretical fits as described in section 4.2.2 A.

Chapter 5 : Investigation of Positive Ions at the Water / CCl_4 Interface

5.1) Introduction

In a further attempt to characterize the water / CCl_4 interface, the dependence of the interfacial SH signal on the presence of small ions was examined. To investigate this, hydrochloric acid was added to the water. A change in the SH signal occurred. To understand the nature of the SH signal, it was monitored while adding sodium chloride (NaCl) and lithium chloride (LiCl). The details of these experiments and the results that were obtained are discussed in the next few sections.

5.2) Ion Adsorption at the Water / CCl_4 Interface

5.2.1) Water Acidity and the Water / Carbon Tetrachloride Interface

The adsorption energetics of small ions at the water / CCl_4 interface were examined. Additions of 0.007 M hydrochloric acid (HCl) were made to the water phase defining the neat interface and the SH signal was monitored. It is the nature of the acid to be ionized in solution. An adsorption study was carried out by examining the SH signal versus the bulk HCl concentration.

Figure 5.1 illustrates the concentration dependence of the SH signal at the neat interface upon addition of HCl to the bulk. The squares represent experimental data and the line is a best fit based on the Frumkin isotherm (as will be discussed in the next section). The plot is the square root of the second harmonic signal versus the concentration. Recall that the square root of the second harmonic signal is proportional to the number of molecules at the interface according to equation (4). As in previous figures, the error bars were determined by repeating the SH intensity measurements at particular concentrations multiple times to determine the reproducibility. The uncertainty associated with these was then taken to be representative of the uncertainty in data displaying comparable signal levels.

It should be noted that when the surface coverage reaches 85% (θ = 0.85), the bulk concentration was measured to be 6.93 x 10^{-6} M.

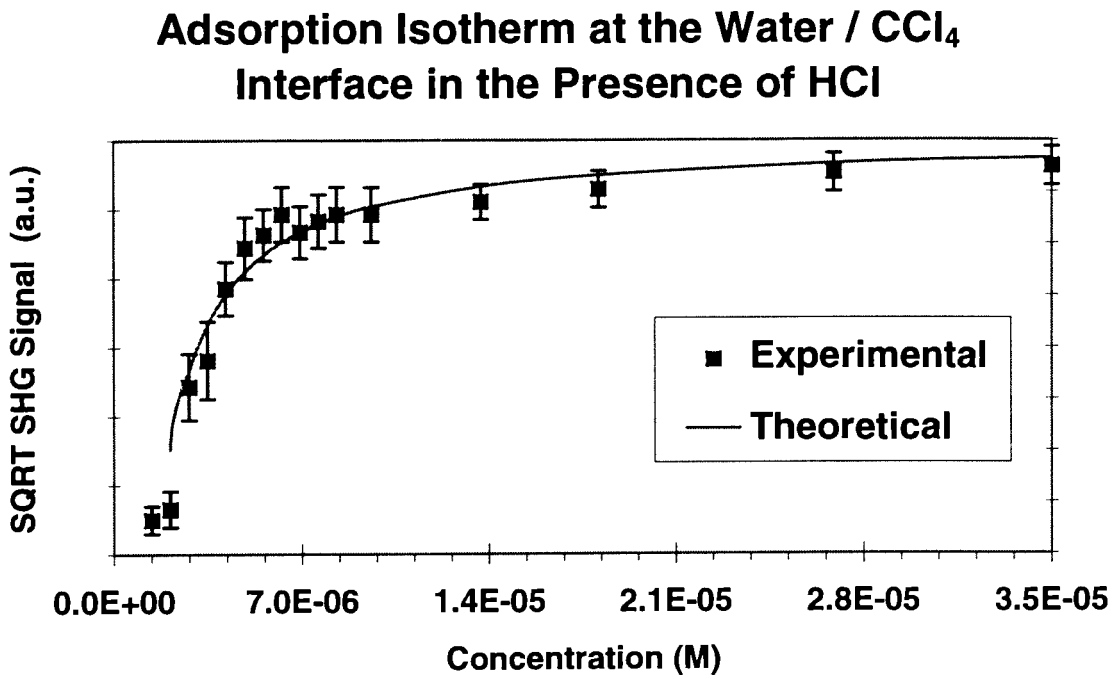

Figure 5.1 : Adsorption Isotherm for the water / CCl_4 interface in the presence of HCl. Squares represent experimental data. Line is a best fit determined by the Frumkin isotherm.

5.2.2) The Frumkin Isotherm

Unlike the case of pNA and its cation, the adsorption isotherm for the interface in the presence of HCl, does not obey the theoretical Langmuir

isotherm. Remember that one of the assumptions of the Langmuir isotherm is that the molecule's ability to be adsorbed is independent of the occupation of neighboring sites.[28] This implies that there are no interactions between the molecules. One would expect, however, that small ions like H^+ and Cl^-, at the interface may possess strong interionic interactions. In this case, the Langmuir isotherm does not provide a good model for interfacial adsorption. A variation of the Langmuir isotherm, the Frumkin isotherm, does take into consideration the attraction or repulsion of adsorbed species and is often used successfully to model the adsorption of ions on metal electrodes.[30] The Frumkin isotherm incorporates a term called the attraction coefficient. If the ions attract each other, the coefficient is positive and if the ions repel each other, the coefficient is negative. As one would expect, when the attraction coefficient approaches zero, the Frumkin isotherm approaches the Langmuir isotherm. The formula for the Frumkin isotherm is

$$\beta C = \frac{\theta}{1-\theta} e^{g\theta} \qquad (22)$$

where θ is the surface coverage ($1 \geq \theta \geq 0$), C is the bulk concentration, g is the attraction coefficient and β, the adsorption coefficient, is given by

$$\beta = \exp\left(\frac{-\Delta G^{o}_{ads}}{RT}\right) \qquad (23)$$

When our data was fitted to equation (22) using a nonlinear least squares fitting technique, a combination of an attraction coefficient, g, of -4.41 ± 0.66 and a $\Delta G°_{ads}$ of 1.46 ± 0.64 kcal/mol gave a best fit. Such a large negative g indicates a strong repulsive force at the interface consistent with either adsorption of the hydrogen or the chloride ions. The $\Delta G°_{ads}$ is the driving force for adsorption at the interface. Its small magnitude and positive sign indicates that the concentration of adsorbed species at the interface is smaller than that in solution and that the interfacial concentration of ions is a result of the increase in bulk concentration. The next step is to determine the identity of the adsorbed species. For this purpose sodium chloride and lithium chloride were also investigated.

5.2.3) The Water / CCl_4 Interface in the Presence of Sodium Chloride and Lithium Chloride

The concentration dependence of the SH signal, upon addition of lithium chloride (LiCl) and upon addition of sodium chloride (NaCl) to the water phase defining the bulk, was observed. As in the case of HCl, these adsorption isotherms were fit using the Frumkin model. Figures 5.3 and 5.4 show the dependence of the SH signal on bulk concentration of LiCl and NaCl respectively. The squares represent experimental data and the lines represent best fits based on the Frumkin isotherm.

As in the case of hydrogen chloride, the lithium and sodium chloride have attraction coefficients of -4.37 ± 1.42 and -2.89 ± 1.08 respectively, indicating a strong repulsive force between the adsorbed species and consistent with ionic adsorption. The corresponding Gibbs free energies of adsorption were found to be 1.64 ± 0.52 kcal/mole and 0.54 ± 0.41 kcal/mol for LiCl and NaCl respectively. These results are similar to those seen for HCl. Based on the $\Delta G°_{ads}$, the interfacial ion concentration is less than that for the bulk and that the increase in bulk concentration causes the increase in interfacial ion concentration.

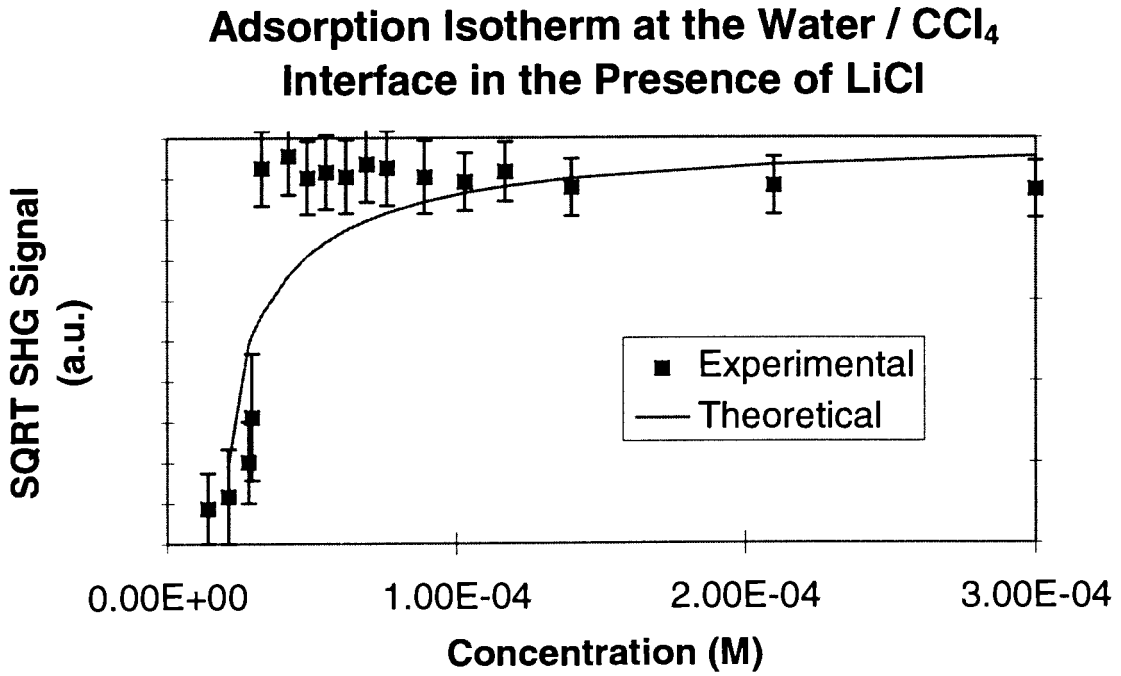

Figure 5.2 : Adsorption Isotherm for the water / CCl_4 interface in the presence of LiCl. Squares represent experimental data. Line is a best fit determined by the Frumkin isotherm.

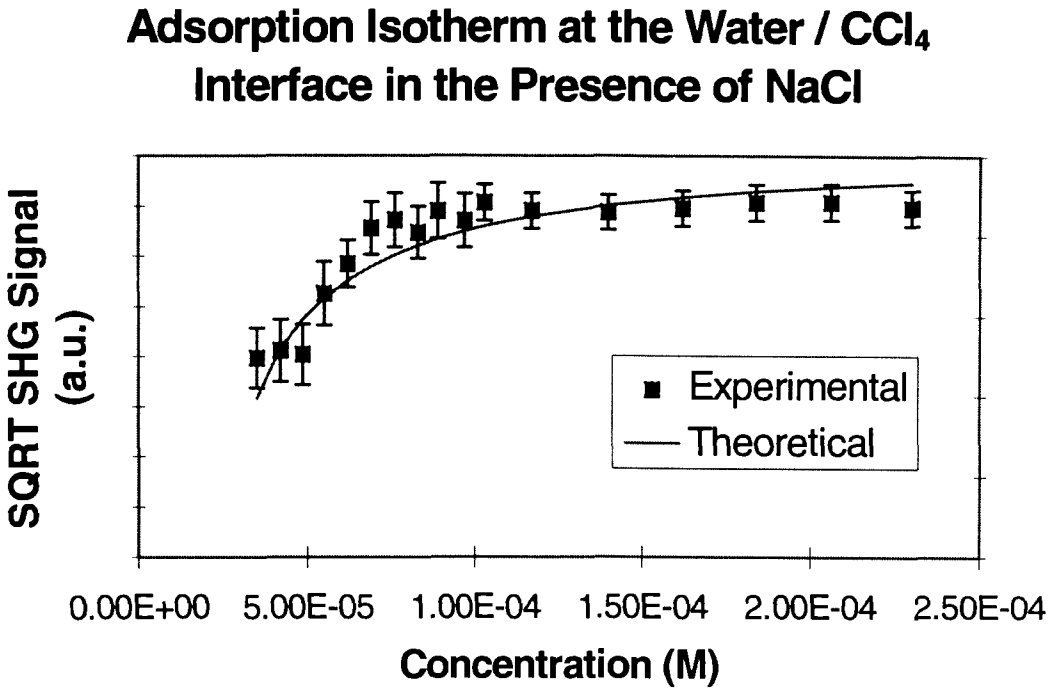

Figure 5.3 : Adsorption Isotherm for the water / CCl_4 interface in the presence of NaCl. Squares represent experimental data. Line is a best fit determined by the Frumkin isotherm.

It is the nature of the acid and the salts to be ionized in solution. Since the SH signal increases with increasing salt concentration and since the only reasonable fits occur when there is a large repulsive factor incorporated, then it can be argued that there is ion adsorption at the interface. The major difference between HCl and the alkali metal chloride salts is the concentration at which adsorption is observed. Recall that for HCl, a surface coverage of 85% was attained at a bulk concentration was 6.93×10^{-6} M. For the cases of LiCl and NaCl there is approximately an order of magnitude increase in bulk concentration

required to reach the point of 85% interfacial coverage. For LiCl when $\theta = 0.85$, the bulk concentration was 3.5×10^{-5} M. For NaCl when $\theta = 0.85$, the bulk concentration was 7.5×10^{-5} M. This large variation in signal with the nature of the cationic species strongly argues that the change in the signal observed is due to a cation effect and not the chloride ions. The behavior of the chloride species remains unclear but more studies must be completed with larger alkali metal chloride salts to form a definite conclusion on this.

5.3) Second Harmonic Polarization Dependence on Cationic Adsorption at the Water / CCl_4 Interface

When HCl, LiCl or NaCl is added to the bulk water the SH signal generated at the interface increases. Since the SHG technique is sensitive to the degree of interfacial polarization and its anisotropy, this observation indicates that some degree of interfacial polarization has occurred. Comparing the increases in SH signal of the HCl, LiCl, and the NaCl argues that the polarization is cation dependent. In order to understand the nature of the SH response further, we have examined the polarization dependence of the SHG.

Figure 5.4 shows the SH polarization curves observed for a bulk HCl concentration of 2.70×10^{-4} M. While varying the polarization of the input light, the SH response was monitored. The filled circles represent the experimental

data for the p-polarized signal, the empty circles represent the experimental data for the s-polarized signal. The lines represent theoretical fits. The error in these points is less than ten percent in the y direction and two degrees or less in the x direction. The uncertainty associated with these points was determined by repeating measurements to determine their reproducibility.

Figures 5.5 and 5.6 show the orientation curves for 3.0×10^{-4} M LiCl and 1.4×10^{-4} M NaCl, respectively. The symbols and the errors are as previously explained for the HCl case. As can be noted in all three polarization curves, the p - polarized signals all have a maximum at $80° + n(90)°$, where n = 0, 1, 2, 3. This is the same phase that was observed for pNA and the opposite phase observed for the neat interface.

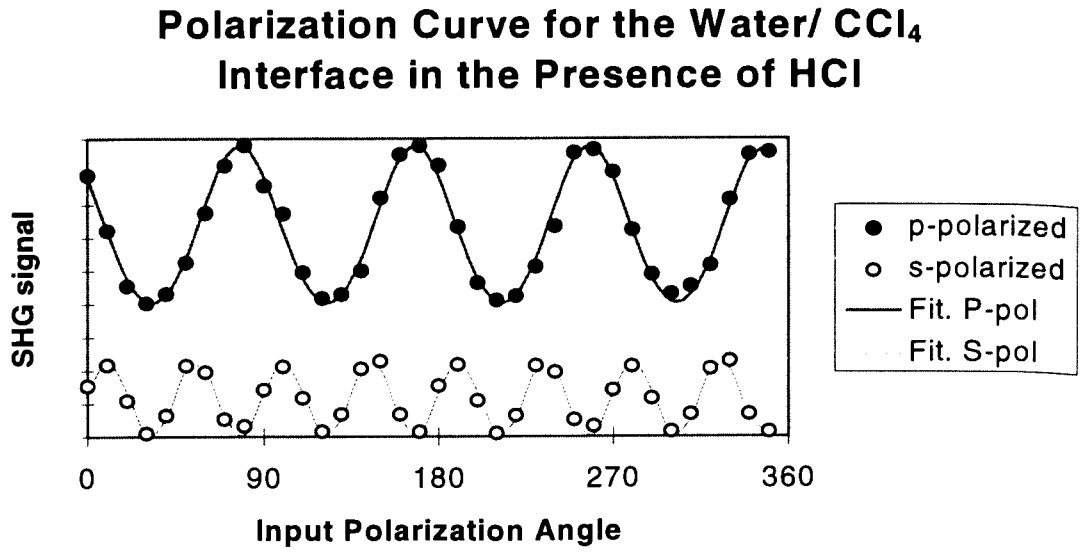

Figure 5.4: Orientation curves for HCl (concentration = 2.7 x 10^{-4} M) of s-and p-polarized SH signal, where filled circles represent p-polarized and hollow circles represent s-polarized. Lines represent theoretical fits. The ratio of $\chi_{xxz}:\chi_{zxx}:\chi_{zzz}$ is $1.0 \pm 0.17 : 1.3 \pm 0.16 : 1.0 \pm 0.12$.

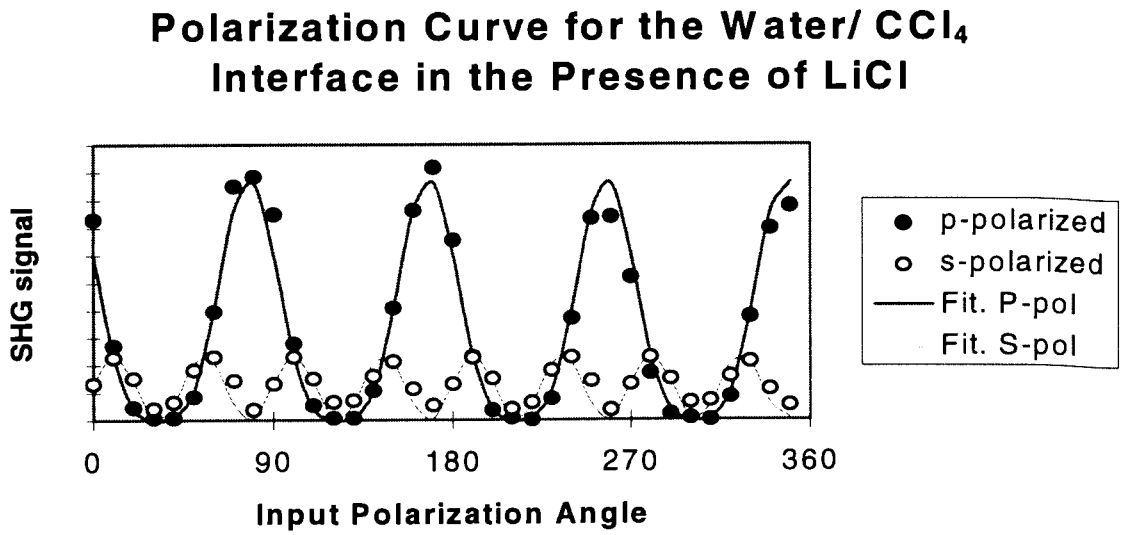

Figure 5.5: Orientation curves for LiCl (concentration = 3.0 x 10^{-4} M) where filled circles represent p-polarized and hollow circles represent s-polarized. Lines represent theoretical fits. The ratio of $\chi_{xxz}:\chi_{zxx}:\chi_{zzz}$ is $1.0 \pm 0.12 : 1.15 \pm 0.28 : 1.98 \pm 0.34$.

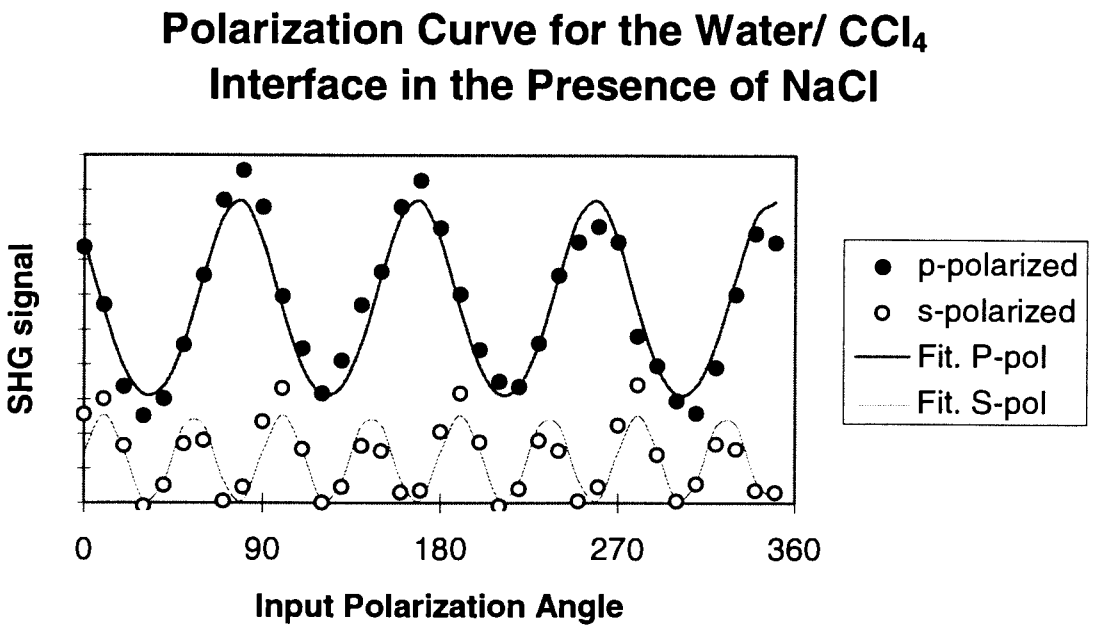

Figure 5.6: Orientation curves for NaCl (concentration = 1.4 x 10^{-4} M) where filled circles represent p-polarized and hollow circles represent s-polarized. Lines represent theoretical fits. The ratio of χ_{xxz}:χ_{zxx}:χ_{zzz} is $1.0 \pm 0.12 : 1.1 \pm 0.28 : 2.0 \pm 0.34$.

5.4) Interface Structure

We would like to understand the nature of our signal. This is very complicated and it is useful to discuss several possibilities as to how the signal is generated. Figure 5.7 is a schematic representation of various possibilities.

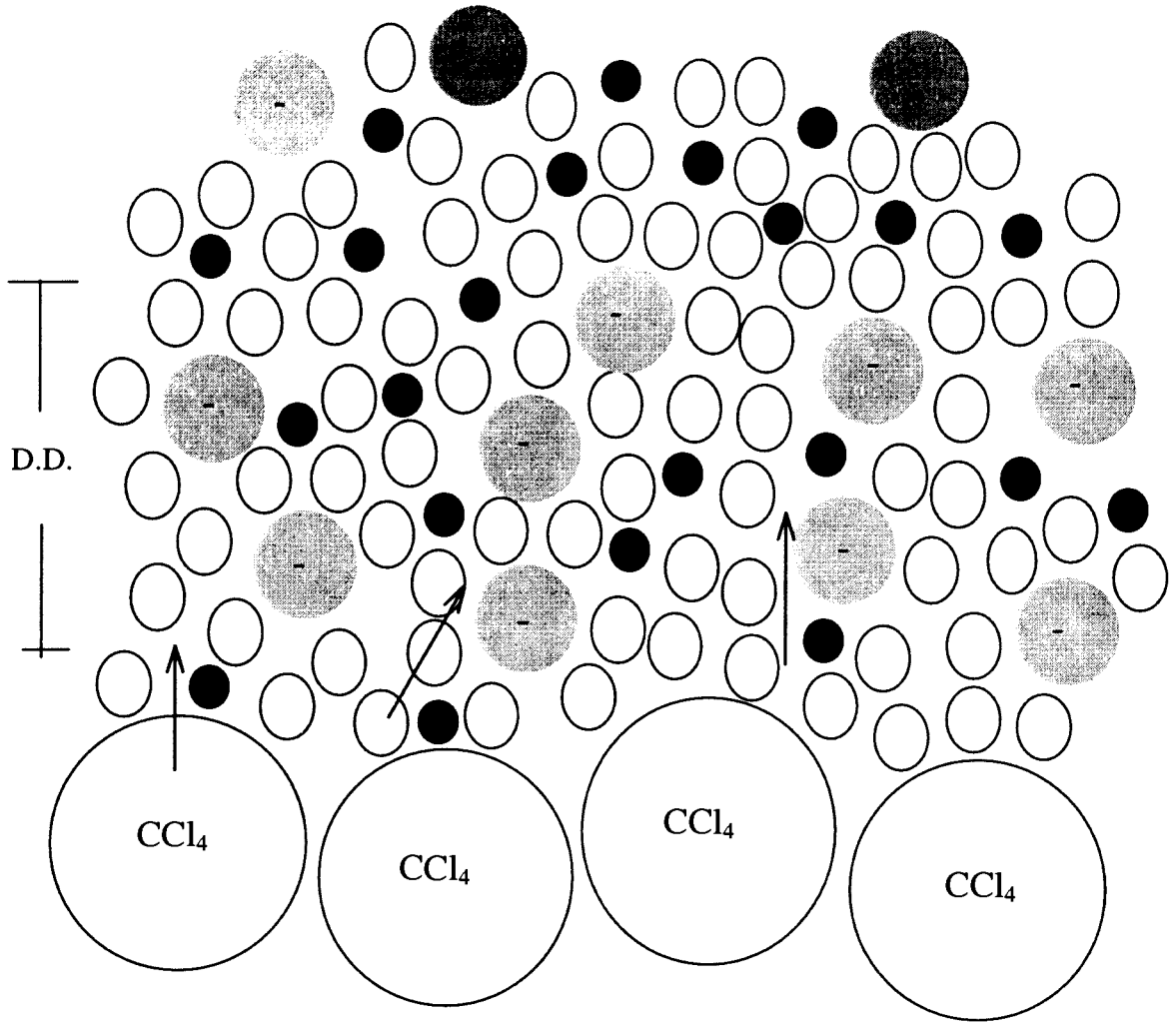

Figure 5.7: Schematic representation of the interface. The gray circles are negative ions, the small black circles are positive ions and the ovals are water. Arrows represent possible dipoles. D.D. represents the diffuse double layer.

We have determined through our adsorption studies that the change in signal is a cationic effect. There are several possible ways that this may be

taking place. One possibility is that ion pairs are forming at the interface and creating an interface polarization as depicted in figure 5.7. Another possibility is that the cation can interact with a chlorine from the CCl_4 and a small polarization arises, also depicted in figure 5.7. In both of these cases, what is called a diffuse double layer is likely to have formed and an electric field induced SH signal is observed. The water solution is thought to be made up of layers. The layer closest to the interface contains solvent and solute molecules, specifically ions, and is said to be specifically adsorbed. The next layer is one that contains nonspecifically adsorbed species, for example counterions. This layer is called the diffuse double layer [30], and is represented in figure 5.7. In the case of a liquid - liquid interface, there is a possibility of having two such diffuse layers, one in each phase. [2] Although this is a possibility, it would not have a huge effect in our particular case because the water phase would much more readily solvate the ions. The dielectric constant for water is approximately 80, compared to that of CCl_4 approximately 2.24. [31]

Another possible reason for the increase in signal upon addition of ions may be the reorganization of the water molecules to solvate the ions. The signal described in chapter 3 for the neat interface was extremely small due to the unique order at the interface. This order is disrupted when ions are placed in solution and the signal increases. This might be a result of the reorganization of the water molecules to accommodate the ions. Varying the size of the ion may lead to more or less reorientation of the water molecules causing the signal to increase or decrease.

Knowing that this is a cation effect and that it is an electric dipole induced SH signal leaves open the possibility for future experiments to learn more about the electric field component without the molecular component. A method of doing this is to perform an absolute molecular orientation measurement to determine the phase of χ, by comparing the signal generated by the sample compared to the signal generated from a reference. [29]

Chapter 6 : Conclusion

Using second harmonic generation, we have studied the structure and adsorption at the water / carbon tetrachloride liquid - liquid interface. First, the neat interface was examined by carrying out polarization dependent studies. From these studies the values for the interfacial susceptibilities were determined and upon analysis it was concluded that a large fraction of the interfacial water molecules lie with their dipole parallel to the interface.

Second harmonic generation was then used to study the adsorption energetics and the averaged orientation of an organic probe molecule, p-nitroaniline. p-Nitroaniline showed a large negative Gibbs free energy of adsorption (-9.48 kcal/mol), suggesting a preference for these molecules to reside at the interface. It was also found that the molecules have a strong orientation preference corresponding to an averaged orientation where the symmetry axis of pNA is at 48° $\pm$ 2° with respect to the surface normal. The pH dependence of p-nitroaniline was also examined to learn about the adsorption energetics and orientation of the p-nitroaniline ion. The repulsions caused by ion formation were insufficient to perturb the orientation observed for neutral pNA. The Gibbs free energy of adsorption decreased significantly in magnitude to -6.62 kcal/mol. This increase is the result of the extra work involved in bringing an ion from a solvated state to an interface where it could not be solvated as

well, and by the extra work involved in bringing a charged species to an already charged interface.

In addition, the water / CCl_4 interface was further characterized by the investigation of the adsorption of small ions, namely hydrogen, lithium, and sodium. The Gibbs free energy of adsorption were small positive numbers for all of the ions, indicating a preference for being in solution. The adsorption of the ions indicated a size dependence but further studies must be carried out to form a definite conclusion on this. The nature of the SH response in the case of small ion adsorption is a result of an electric field induced process and was effected by the reorientation of the water molecules to solvate these ions.

Works Cited

1) K. B Eisenthal, *Acc. Chem. Res.*, **26**, 636, (1993)

2) A. G. Volkov, D. W. Deamer, *"Liquid-Liquid Interfaces: Theory and Methods"*, (Chapters 4 and 6), CRC Press, New York, 1996

3) F. Zernicke, J. E. Midwinter *"Applied Nonlinear Optics"*, John Wiley and Sons Inc., (Chapter 1), Toronto, 1973

4) P. N. Prasad, D. J. Williams, *"Introduction to Nonlinear Optical Effects in Molecules and Polymers"*, (Chapter 1), John Wiley and Sons Inc., Toronto, 1991

5) T. F. Heinz, C. K. Chen, D. Richards, and Y. R. Shen, *Phys. Rev. Lett.*, **46**,1010, (1981)

6) D. A. Higgens, M. B. Abrams, S. K. Byerly and R. M. Corn, *Langmuir,* **8**, 1994, (1992)

7) E. V. Stizman, K. B. Eisenthal, *J. Phys. Chem.*, **90**, 2831, (1989)

8) E. N. Svendsen, C. S. Willand, A. C. Albrecht, *J. Chem. Phys.,* **83**, 5760, (1985)

9) S. R. Marder, D. N. Beratan, L. T. Cheng, *Science,* **252**, 103, (1991)

10) T. F. Heinz, H. W. K. Tom, Y. R. Shen, *Phys. Rev. A,* **28(3)**, 1883, (1983)

11) D. A. Higgens, R. M. Corn, *J. Phys. Chem.*, **97**, 489, (1993)

12) R. R. Naujok, D. A. Higgens, D. G. Hankan, and R. M. Corn, *J. Chem. Soc. Faraday Trans.*, **91(10)**, 1411, (1995)

13) H. J. Paul and R. M. Corn, *J. Phys. Chem. B,* **101**, 4494, (1997)

14) K. Bhattacharyya, A. Castro, E. V. Sitzmann, and K. B. Eisenthal, *J. Chem. Phys.*, **89(5)**, 3376, (1988)

15) A. Castro, K. Bhattacharyya, and K. B. Eisenthal, *J. Chem. Phys.*, **95(2)**, 1310, (1991)

16) J. C. Conboy, J. L. Daschbach, and G. L. Richmond, *J. Phys. Chem.*, **98**, 9688, (1994)

17) T. Rasing, and Y.R. Shen, *Phys. Rev. A,* **31(1)**, 537, (1985)

18) K. Bhattacharyya, E. V. Sitzmznn, K. B. Eisenthal, *J. Chem. Phys.*, **87(2)**, 1442, (1987)

19) M. C. Goh, J. M. Hicks, K. Kemmitz, G. R. Pinto, T. F. Heinz, K. Bhattacharyya, and K. B. Eisenthal, *J. Phys. Chem.*, **92**, 5074, (1988)

20) S. R. Meech, K. Yoshihara, *Chem. Phys. Lett.*, **174**, 423, (1990)

21) S. R. Meech, K. Yoshihara, *J. Phys. Chem.*, **94**, 4913, (1990)

22) N. J. Harrwick, *"Internal Reflection Spectroscopy"*, Interscience Publishers, (Chapter 1), New York, 1967

23) J. Israelachvili, *" Intermolecular and Surface Forces",* (Chapter 8), Academic Press, Toronto, 1992

24) B. U. Felderhof, A. Bratz, G. Marowsky, O. Roders, and F. Sieverdes, *J. Opt. Am. B.*, **10(1)**, 1824, (1993)

25) G. D. Purvis, R. J. Bartlett, *J. Phys. Rev. A*, **23**, 2429, (1981)

26) Q. Du, E. Fresysz, Y. R. Shen, *Science,* **264**, 826, (1994)

27) Q. Du, R. Superfine, E. Freysz, Y. R. Shen, *Phys. Rev. Lett.*, **10(15)**, 2313, (1993)

28) P. W. Atkins, *" Physical Chemistry",* (Chapter 28), W. H. Freeman and Company, New York, 1994

29) A. Ulman, *"Characterization of Organic Thin Films",* (Chapter 12), Manning Publications Co., Greenwich, CT, 1995

30) A. J. Bard, L. R. Faulkner, *"Electrochemical Methods: Fundamentals and Applications",* (Chapter 12), John Wiley and Sons, Toronto, 1980

31) D. R. Lide, *"CRC Handbook of Chemistry and Physics",* CRC Press, 1992

32) R. H. Harris, *" Nuclear Magnetic Resonance Spectroscopy",* (Chapters 4 and 6), Longman Scientific and Technical, New York, 1994